

NPS ARCHIVE  
1969  
DOHERTY, B.

DESIGN OF A COBALT-60 FUELED  
THERMIONIC POWER SUPPLY

by

Brian J. Doherty

LIBRARY  
NAVAL POSTGRADUATE SCHOOL  
MONTEREY, CALIF. 93940

DESIGN OF A COBALT-60 FUELED  
THERMIONIC POWER SUPPLY

by

Brian J. Doherty  
B. S., United States Naval Academy  
(1965)

Submitted in Partial Fulfillment  
of the Requirements for the  
Degrees of Master of  
Science  
and  
Nuclear Engineer  
at the  
Massachusetts Institute of  
Technology  
June, 1969

1170 ARCHIVE  
1067  
LUCAS (K)

~~thesis~~ D634

## DESIGN OF A COBALT-60 FUELED THERMIONIC POWER SUPPLY

by

Brian J. Doherty

Submitted to the Department of Nuclear Engineering on June 30, 1969 in partial fulfillment of the requirements for the degrees of Master of Science and Nuclear Engineer.

### ABSTRACT

The objective of this thesis was to design a practical thermionic power supply which would use cobalt-60 as a fuel and which would provide 500 watts of electric power over a three year operating period.

In order to make the cobalt-60 fuel, which has a low melting point, compatible with the high temperature required for efficient operation of a thermionic converter, a low temperature fuel concept was employed. This meant that the fuel would be insulated from the converter heat source by a multi-foil thermal insulation. The multi-foil insulation uses refractory metal foils separated by thin layers of refractory oxide particles to provide a highly efficient and compact thermal insulation. With this design it was desirable to minimize the gamma self absorption of the fuel. Most of the effort in this thesis was directed toward the optimization of the fuel supply. The final design uses fuel elements which are in the form of hollow cylinders and which have a thermal efficiency of 75.6%.

A power flattening device which operates on a moveable fuel concept was designed to overcome the problems posed by the relatively short half life of cobalt-60.

The power supply was designed for terrestrial applications; accordingly it was not subjected to severe weight limitations. Nevertheless, every effort was made to keep its weight and size within reasonable limits. The power supply was also designed so that it could operate automatically, unattended, for the three year lifetime. An additional design criteria was that no significant advance in the present state of the art be required for the design to be feasible.

The final design uses five thermionic converters operating at a fixed power point and a DC-DC regulated converter to provide 500 watts of electric power at 28 volts. The overall efficiency of the power supply system is 9.7%.

Thesis Supervisor: E. P. Gyftopoulos  
Title: Professor of Nuclear Engineering



## TABLE OF CONTENTS

Abstract	ii
Table of Contents	iii
List of Figures and Tables	v
CHAPTER 1 INTRODUCTION	
1.1 Objective	1
1.2 Design Concept	1
1.2.1 Fuel Requirements	1
1.2.2 Low Temperature Fuel Concept	2
1.3 Preliminary Design Considerations	4
1.4 Further Design Refinements	5
CHAPTER 2 SELECTION OF THERMIONIC CONVERTER DESIGN	
2.1 General Remarks	8
2.2 Thermionic Converter Performance Characteristics	8
2.2.1 Performance Characteristics Used As Design Basis	8
2.2.2 Intrinsic Efficiency	9
2.2.3 Emitter And Collector Operating Temperatures	15
2.2.4 Output Voltage	16
2.3 Thermionic Converter Designs Compatible With Power Flattening Requirements	18
2.3.1 Power Flattening Requirements	18
2.3.2 Converter Operation With Varying Cesium Reservoir Temperature	18
2.3.3 Operation At A Fixed Power Point	21
CHAPTER 3 FUEL ELEMENT OPTIMIZATION	
3.1 General Remarks	26
3.2 Fuel Element Configuration	26
3.3 Energy Losses To The Fuel Elements	29
3.4 Fuel Element Efficiency	30
3.5 Calculation Of $E_{\beta}$	30
3.6 Calculation Of $E_{\gamma F}$	31
3.7 Calculation Of $E_{\gamma C}$ And $E_{\gamma I}$	31
3.8 Calculation Of $E_{S\gamma}$	36
3.9 Calculation Of $Q_I$	38
3.10 Evaluation Of Specific Fuel Elements	40
CHAPTER 4 SHIELDING	
4.1 General Remarks	50
4.2 Method For Calculation Of Shield Thickness	50
4.3 Shield Design	53
CHAPTER 5 POWER CONDITIONING	
5.1 General Remarks	59





## TABLE OF CONTENTS (CONT. )

5.2	Operating Principle Of The Power Flattening Mechanism	61
5.3	Fuel Rod Positioning Mechanism	61
5.4	Initial Fuel Rod Position	62
5.5	Operation Of The Fuel Positioning Mechanism	63

### CHAPTER 6 ADDITIONAL DESIGN CONSIDERATIONS

6.1	General Remarks	65
6.2	Lead Losses	65
6.3	Insulation And Support Of The Emitter Heat Source	66
6.4	Modifications Requires To Fuel Element Design	67
6.5	Electrical Insulation Of Emitter And Collector	68
6.6	Radiator Design	70

### CHAPTER 7 SUMMARY AND CONCLUSIONS

7.1	Design Summary	73
7.2	Conclusions	73

BIBLIOGRAPHY	78
--------------	----



## LIST OF FIGURES AND TABLES

Figure 1.2.2.1	
Schematic Power Supply Design	3
Figure 2.2.1.1	
Thermionic Converter Output Voltage Characteristics	10
Figure 2.2.1.2	
Thermionic Converter Intrinsic Efficiency Characteristics	11
Figure 2.2.1.3	
Thermionic Converter Output Power Characteristics	12
Figure 2.2.1.4	
Thermionic Converter Intrinsic Efficiency Characteristics	13
Figure 2.2.1.5	
Thermionic Converter Output Power Characteristics	14
Figure 2.2.4.1	
Representative DC-DC Converter Efficiencies	17
Table 2.3.2.1	
Characteristics Of Converter With Variable Cesium Reservoir Temperature	22
Table 2.3.3.1	
Characteristics Of A Converter Operating At A Constant Power Point	24
Figure 3.2.1	
Cross Section Of Solid Fuel Element	27
Figure 3.2.2	
Cross Section Of Tubular Fuel Element	28
Figure 3.6.1	
Gamma Self Absorption Factor	32
Figure 3.7.1	
Geometry Used In The Calculation Of $I_p$	34
Figure 3.7.2	
Normalized Intensity Of Absorbed Radiation	35
Figure 3.8.1	
Isotropic Source Gamma Albedo For Tungsten	37
Figure 3.9.1	
W-ThO <sub>2</sub> Multi-Foil Insulation Thermal Conductivity	39
Figure 3.10.1	
Comparison Of Solid Fuel Element Efficiencies	41
Table 3.10.1	
Components Of Heat Loss In Solid Cylinder Fuel Elements	43
Table 3.10.2	
Components Of Heat Loss For Different Fuel Element Configurations	44
Table 3.10.3	
Components Of Heat Loss In Tubular Fuel Elements	45
Figure 3.10.2	
Comparison Of Solid and Tubular Fuel Element Efficiencies	46
Figure 3.10.3	
Tubular Fuel Element Efficiency	47



## LIST OF FIGURES AND TABLES (CONT. )

Figure 4. 2. 1	
Geometry Used In The Calculation Of Shielding	51
Figure 4. 3. 1	
Emitter Heat Source	54
Table 4. 3. 1	
Required Shiel Thicknesses	55
Figure 4. 3. 2	
Cross Section Of Shield Assembly	57
Figure 5. 1. 1	
Power Flattening Mechanism	60
Figure 6. 5. 1	
Thermionic Converter Configuration	69
Table 7. 1. 1	
Final Design Summary	75



# CHAPTER 1

## INTRODUCTION

### 1.1 OBJECTIVE

The objective of this thesis is to design a thermionic power supply which will be fueled with cobalt-60 and which will provide 500 watts of electric power over a three year operating period. The design lifetime of three years was chosen because the required life of many operational radioisotope power supplies is between one and five years. (Reference 1.1)

Most of the effort in this thesis has been directed toward the optimization of the fuel supply and toward the power flattening requirements. The final design has been formulated so that no significant advances in the present state of the art are required for it to be feasible.

The power supply was designed for terrestrial applications, accordingly it is not subjected to severe weight limitations. Nevertheless every effort has been made to keep weight and size within reasonable limits. The power supply was also designed so that it could operate automatically, unattended, for the three year lifetime.

### 1.2 DESIGN CONCEPT

#### 1.2.1 FUEL REQUIREMENTS

In order to operate a thermionic converter efficiently the temperature of the thermionic emitter must be at least 1500°C. Most design concepts for radioisotope power generators require that the isotope fuel operate at temperatures higher than the thermionic emitter temperature in order for heat transfer to occur. Difficulties associated with the operation of isotope fuel at these high temperatures have proven to be





the primary deterrent to the use of isotope fueled thermionic converters.

The relative low cost and high power density of cobalt-60, compared to other isotope fuels such as strontium-90, make it attractive as a fuel. (Reference 1.2) However, the melting point of cobalt-60 is  $1495^{\circ}\text{C}$ , and that is significantly below the melting point required for a useful thermionic converter fuel. To make this isotope compatible with thermionic converter requirements, alloys of cobalt and rhenium have been tested in an attempt to produce an isotopic fuel form with a high melting point. This approach has not been entirely successful. One of its major drawbacks is that the alloy must be formed after the cobalt has been irradiated.

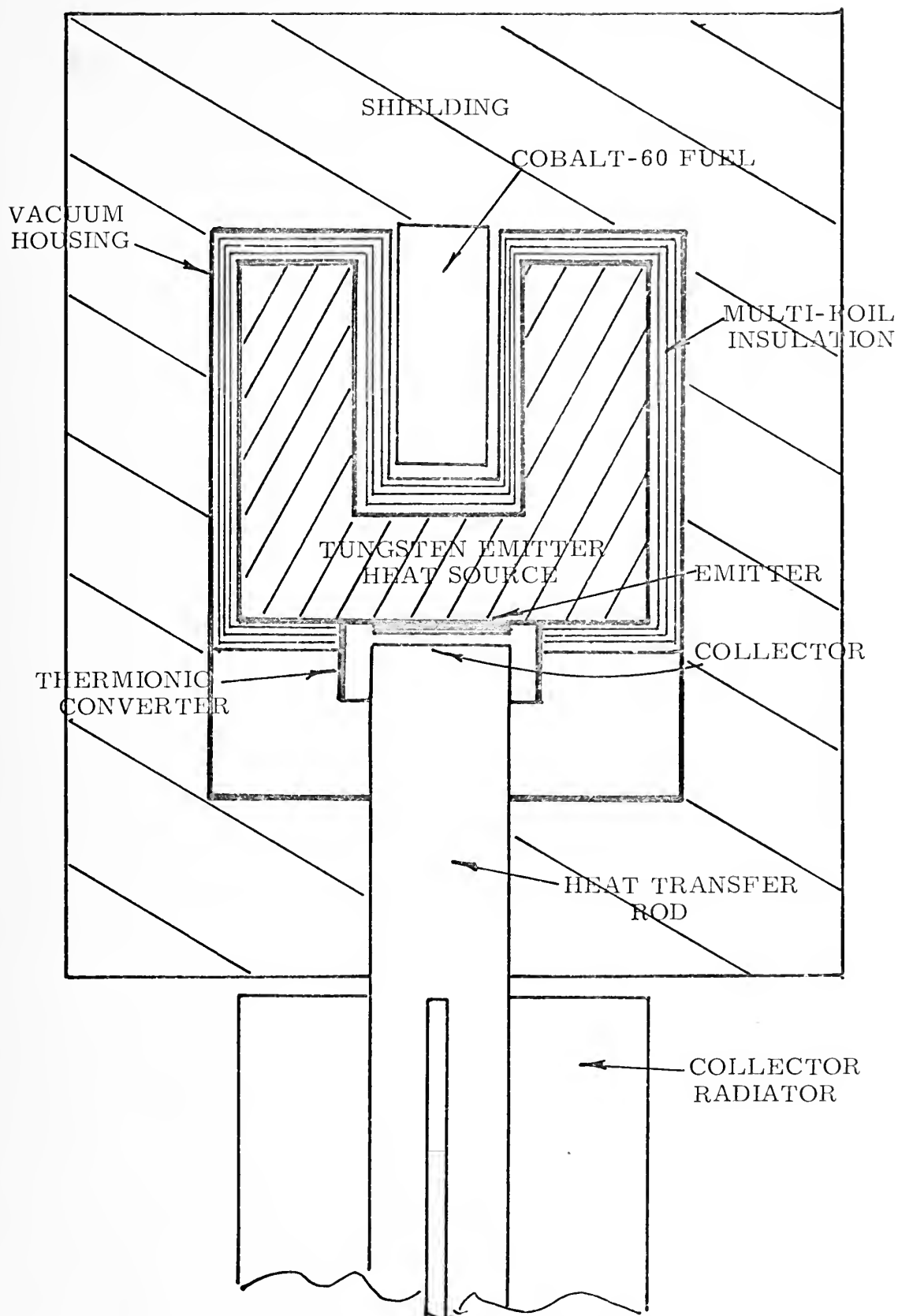
### 1.2.2 LOW TEMPERATURE FUEL CONCEPT

Considering the facts mentioned above the choice of cobalt-60 as a fuel for a thermionic power supply appears at best to be illadvised. However, an interesting concept has been proposed which will allow an isotope which emits energetic gamma radiation to be used as a fuel. (Reference 1.3)

This design concept is presented schematically in Figure 1.2.2.1. The design proposes to thermally insulate the gamma source (the isotope fuel, cobalt-60 in this case) from a surrounding medium of gamma absorber. The gamma radiation from the fuel would be absorbed and converted into heat by the gamma absorber. The gamma absorber would then act as the heat source for the thermionic emitter.

Since the cobalt-60 is thermally insulated from the emitter heat source (gamma absorber), it can operate at a temperature lower than the temperature of the emitter heat source and lower than its own melting point. This design concept has recently become feasible due to the





SCHEMATIC POWER SUPPLY DESIGN

FIGURE 1.2.2.1



development of a high temperature multi-foil insulation which uses refractory metal foils separated by thin layers of refractory oxide particles to provide a highly efficient and compact thermal insulation.

(Reference 1. 4)

### 1. 3 PRELIMINARY DESIGN CONSIDERATIONS

Several additional design requirements are illustrated in Figure 1. 2. 2. 1. Some of these have been selected for convenience, others are required by the operating conditions.

Since the high operating temperature of the emitter heat source required the use of a refractory material, tungsten was selected as the material to be used. The high atomic number of tungsten gives it good gamma absorption properties.

The high temperature of the thermionic converter and its heat source imposes a requirement that the system operate in a vacuum in order to prevent rapid oxidation of the high temperature components. Thus the vacuum housing, shown in Figure 1. 2. 2. 1, was included in the design in order to maintain a vacuum around the high temperature components.

In order to facilitate fabrication of the thermionic converter and heat source assembly it is desirable to delay loading of the isotope fuel until all other steps in the fabrication process have been completed. This procedure will minimize the work which must be performed remotely in a hot cell and thus greatly simplify assembly of the unit. It was therefore decided to locate the fuel outside of the vacuum housing.

Approximately one fifth of the energy transferred from the emitter to the collector of the thermionic converter is removed as electric power. It is thus necessary to provide a means of removing the remainder



of this energy in order to maintain the collector at a constant temperature. A radiator is provided so that the excess energy can be dissipated in the atmosphere. Since the radiator area remains constant throughout the operating period, the collector temperature will be determined by the heat flux to it from the emitter and the output power.

The hard gamma radiation from the cobalt-60 (1.17 and 1.33 Mev per disintegration) requires that the power supply be shielded in order to protect personnel from the ionizing radiation.

Since there will be some heat generated in the fuel a means must be provided to remove the heat so that the fuel will remain at a low temperature. In Figure 1.2.2.1 the heat removal is accomplished by conduction through the shield. As this design was modified, it became necessary to provide the fuel with a radiator assembly similar to the collector radiator.

#### 1.4 FURTHER DESIGN REFINEMENTS

The basic design is now qualitatively set and is represented schematically in Figure 1.2.2.1. In the following chapters the design will be modified in an attempt to both optimize its performance and to remain within limits set by materials and the state of the art.

The thermionic converter design is considered in Chapter 2. A practical output voltage for the power supply is selected and methods of obtaining it discussed. A thermionic converter design is selected and the output power requirements are used to fix the operating point and determine the required input power. Power flattening concepts are investigated and the mode of power flattening selected.

In Chapter 3 the fuel element design is optimized so that the maximum useful energy will be delivered to the emitter heat source. An





optimized fuel element design is selected to meet the converter input power requirements which were determined in Chapter 2.

The shielding requirements are discussed in Chapter 4. The shielding calculations are explained and the shield design is finalized.

Since no power flattening device found was compatible with this design's needs, one was designed. The power flattening mechanism is discussed in Chapter 5.

Chapter 6 contains an explanation of numerous heat losses which degrade the performance of the thermionic converter and cause it to operate at less than the intrinsic efficiency. The effect of these heat losses on the fuel element design is also treated. Several additional design problems which were not treated in detail are summarized.

The final design is summarized in Chapter 7 and conclusions are drawn.



## REFERENCES

- 1.1 Corliss, W.R. and Harvey, D.G., Radioisotopic Power Generation, Englewood Cliffs: Prentice Hall, Inc., 1964.
- 1.2 Hilbom, H.S., "Savannah River Laboratory Isotopic Power and Heat Sources, Part I Co-60," Quarterly Progress Report, July - September, 1967, DP-1129-1.
- 1.3 Dunlay, J.B., "Description of a Cobalt-60 Fueled Thermionic Generator Experiment," Conference Record of the Thermionic Conversion Specialist Conference, October, 1967.
- 1.4 Carvalho, J. and Dunlay, J.B., "Quarterly Progress Report of Research and Development of Vacuum Foil Type Insulation for Radioisotope Power Systems," Thermo Electron Corp., Report No. 4059-109-69, January 20, 1969.



## CHAPTER 2

### SELECTION OF THERMIONIC CONVERTER DESIGN

#### 2.1 GENERAL REMARKS

Thermionic converter performance characteristics (i. e. , output current density, output power density and intrinsic efficiency) are functions of several parameters. These parameters can be varied in a manner such that the desired power output can be obtained using any one of several different parameter combinations. In this chapter a set of performance characteristics, which has been extracted from the literature, is discussed and the reasoning used in fixing the converter operating parameters is explained.

Methods of obtaining a practical voltage output and their effects on converter design are explained. The choice of the method to be used in this power supply design is made.

The problem of power flattening is also treated. Two power flattening concepts are proposed and discussed. Thermionic converters designed to operate using each of the power flattening concepts are discussed and compared.

Finally the thermionic converter design to be used in this power supply is selected.

#### 2.2 THERMIONIC CONVERTER PERFORMANCE CHARACTERISTICS

##### 2.2.1 PERFORMANCE CHARACTERISTICS USED AS DESIGN BASIS

The performance characteristics (i. e. , output current density, output power density and intrinsic efficiency) are functions of the cesium reservoir temperature  $T_R$ , emitter temperature  $T_E$ , collector temperature  $T_C$ , interelectrode spacing and electrode material. In order to select the



operating values of these parameter it is desirable to have data which shows the functional dependence of the thermionic converter performance characteristics on each of the variable parameters.

Figures 2.2.1.1 through 2.2.1.5 show the thermionic converter performance characteristics of a converter with tungsten emitter at 2000<sup>o</sup>K, molybdenum collector and an interelectrode spacing of 7.0 mils as a function of cesium reservoir temperature and collector temperature. These performance characteristics were calculated using an analytical converter model. These theoretical characteristics are in good agreement with corresponding experimental characteristics. The method used to calculate these characteristics is explained in References 2.1 and 2.2.

Although the data presented in Figures 2.2.1.1 through 2.2.1.5 is for an emitter temperature of 2000<sup>o</sup>K, Reference 2.1 provides similar data for emitter temperatures ranging from 1600<sup>o</sup>K to 2100<sup>o</sup>K. As explained below, however, 2000<sup>o</sup>K is the emitter operating temperature and 1000<sup>o</sup>K is the collector operating temperature which were selected for the proposed power supply.

## 2.2.2 INTRINSIC EFFICIENCY

The intrinsic efficiency appears as the ordinate on the graph in Figures 2.2.1.2 and 2.2.1.4; it is defined here so that no confusion will arise.

The intrinsic efficiency  $\eta_i$  of a thermionic converter is defined as the efficiency in the absence of electrode, lead, and structural support losses. This efficiency is independent of detailed converter design considerations and is given by

$$\eta_i = P / (Q_e + Q_i + Q_r + Q_g) \quad (2.2.2.1)$$





## THERMIONIC CONVERTER OUTPUT VOLTAGE CHARACTERISTICS

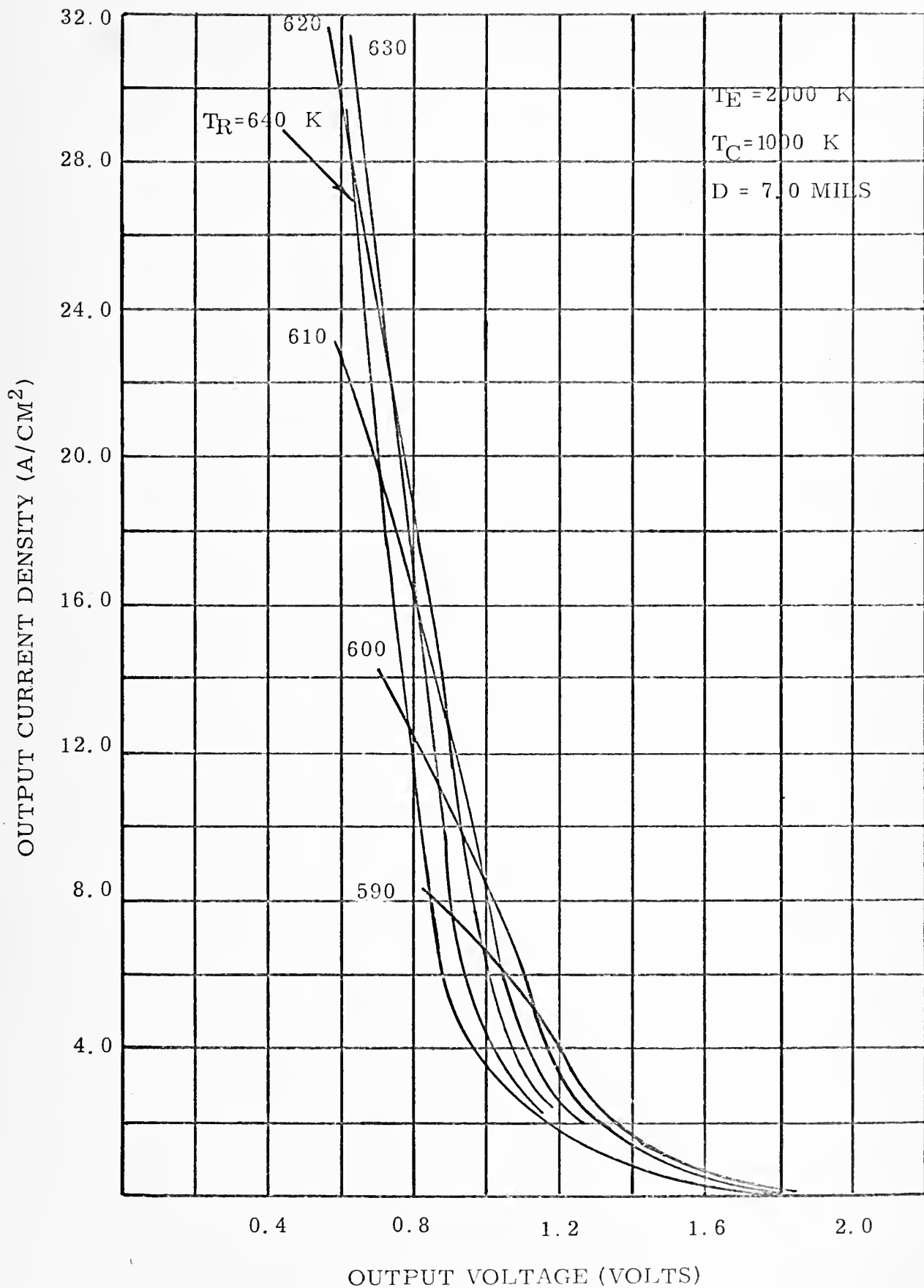


FIGURE 2.2.1.1



## THERMIONIC CONVERTER INTRINSIC EFFICIENCY CHARACTERISTICS

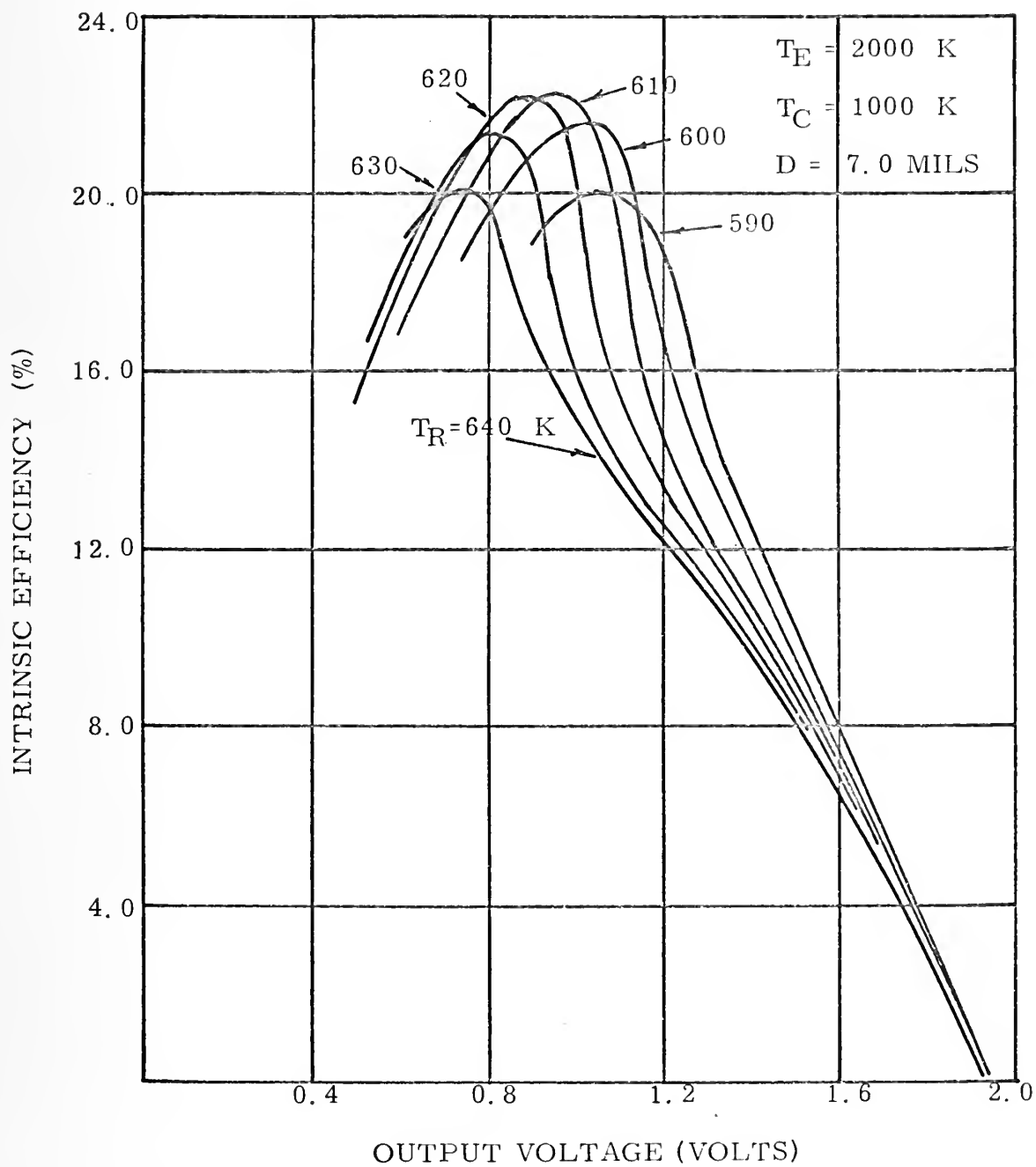


FIGURE 2.2.1.2



## THERMIONIC CONVERTER OUTPUT POWER CHARACTERISTICS

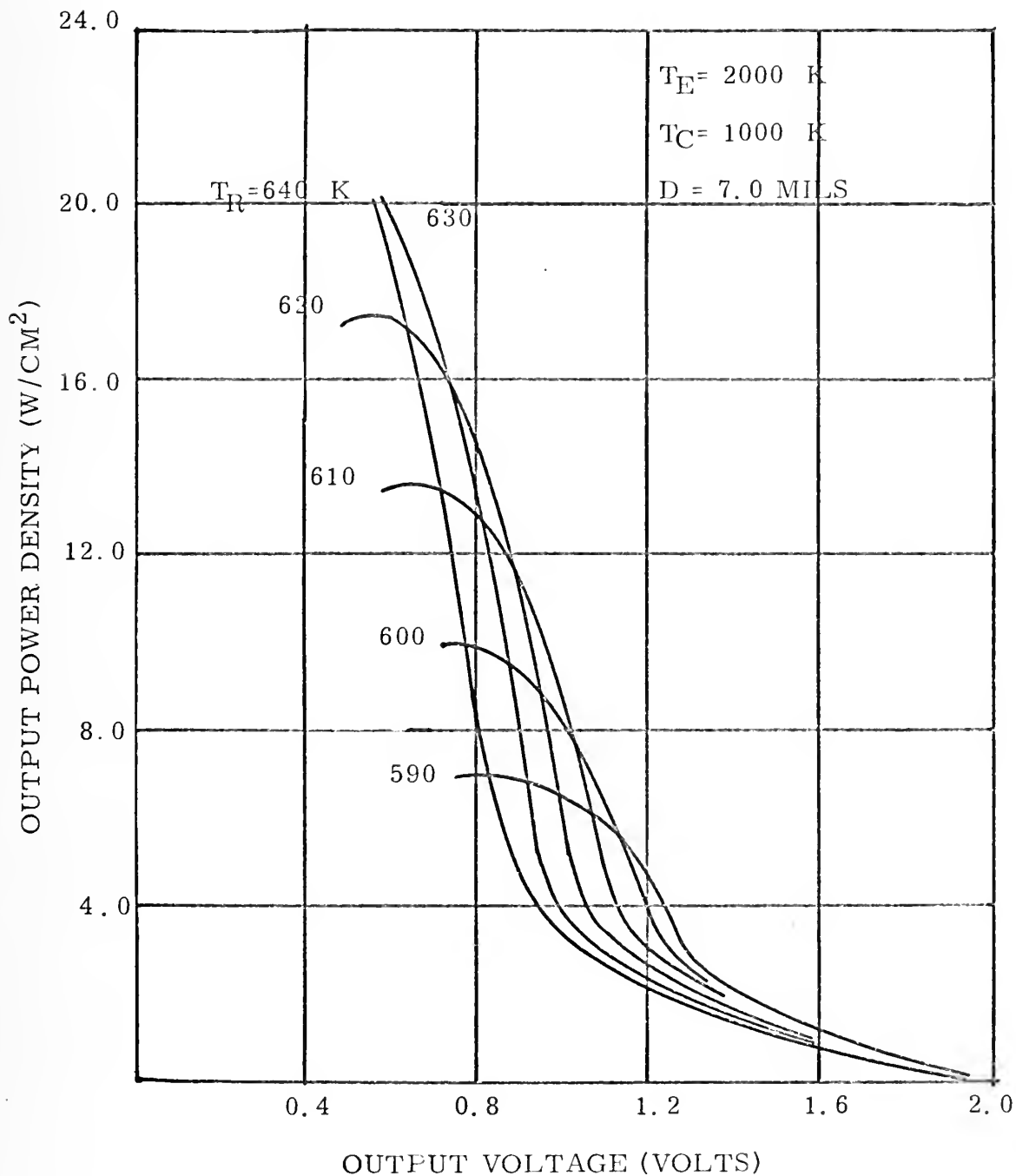


FIGURE 2.2.1.3



## THERMIONIC CONVERTER INTRINSIC EFFICIENCY CHARACTERISTICS

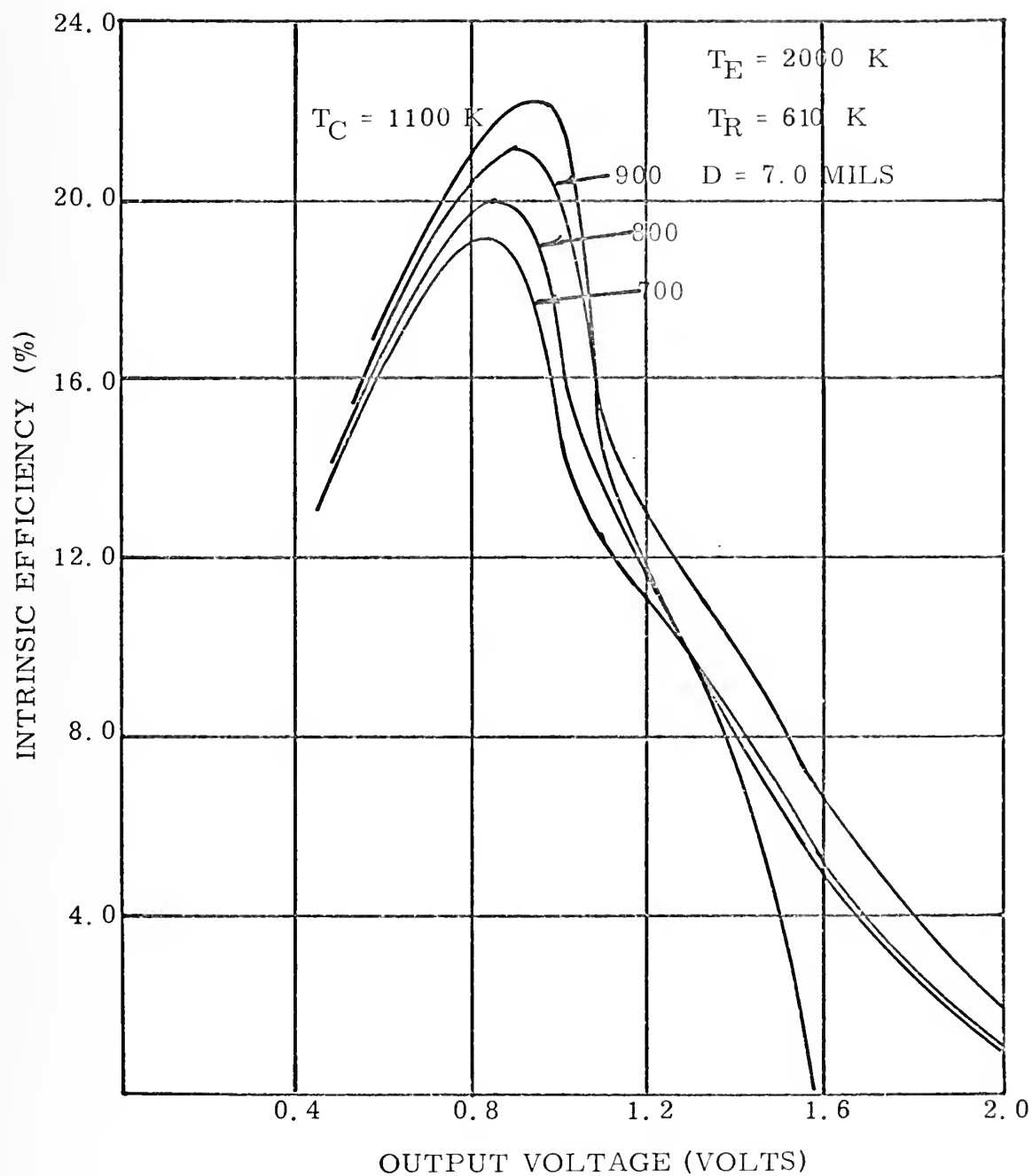


FIGURE 2.2.1.4





## THERMIONIC CONVERTER OUTPUT POWER CHARACTERISTICS

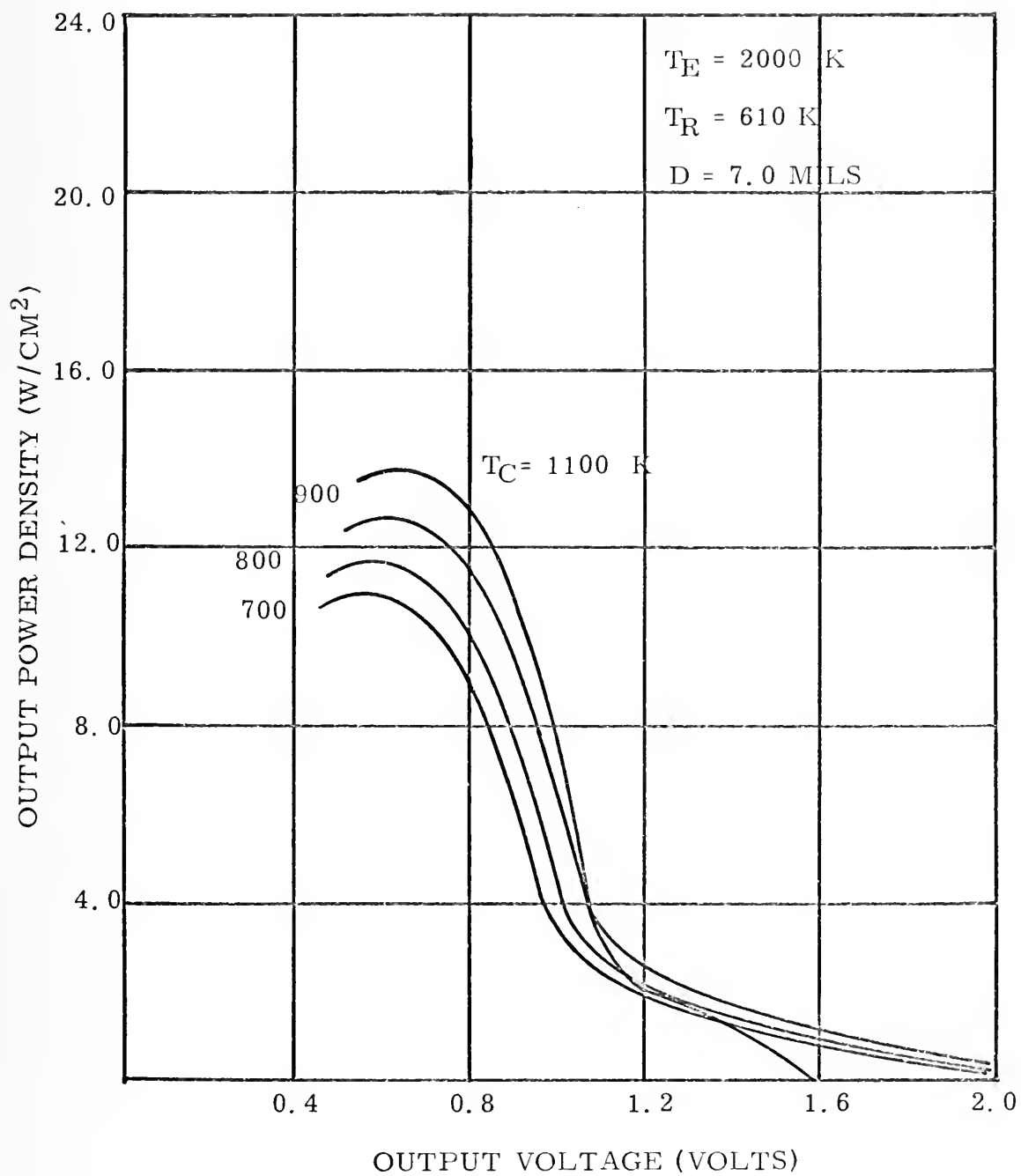


FIGURE 2.2.1.5



where  $P$  is the output power density and  $Q_e$ ,  $Q_i$ ,  $Q_r$  and  $Q_g$  are the heat fluxes removed from the emitter due to electrons, ions, radiation and gas conduction, respectively.

$Q_e$  is by far the most important term and  $Q_r$  is the only other heat flux which is significant.

### 2.2.3 EMITTER AND COLLECTOR OPERATING TEMPERATURES

It is generally true that the efficiency of an optimized thermionic converter increases monotonically with increasing emitter temperature. It is thus desirable to operate the converter at the highest allowable emitter temperature. The highest temperature allowed in the system is limited to  $2270^{\circ}\text{K}$  by the tungsten multi-foil insulation which is used to insulate the fuel elements and the emitter heat source. (Reference 2.3)

The highest temperature to which the multi-foil insulation will be subjected occurs at a point on the emitter heat source at the end farthest from the emitter. Using first design iteration values for heat fluxes and emitter heat source size, it was determined that the maximum allowable emitter temperature would be approximately  $2100^{\circ}\text{K}$ . Since it was expected that further refinement of the design (i. e. necessity to electrically insulate the emitter from its heat source) would lead to a larger temperature drop across the heat source, it was decided that the design would be based on the performance characteristics of a converter with an emitter temperature of  $2000^{\circ}\text{K}$ .

The operating temperature of the collector was selected as  $1000^{\circ}\text{K}$  since this gives the highest intrinsic efficiency for an emitter temperature of  $2000^{\circ}\text{K}$ . Since the collector radiator is fixed in size, the heat flux from the emitter to the collector must be constant in order to maintain a constant



collector temperature for a given electric power output.

#### 2.2.4 OUTPUT VOLTAGE

Much of the equipment which power supplies of this type are designed to power require input voltages on the order of 28 volts. (Reference 2.4) It was therefore decided that in order to be practical this power supply should have an output voltage of 28 volts.

Thermionic converters are classified as low voltage, high current devices. The output of a single thermionic diode is on the order of one volt. Thus, in order to furnish power at the desired 28 volts, many thermionic diodes must be connected in series or the output from a few diodes must be stepped up using a DC-DC converter. The second alternative is more attractive since it requires fewer diodes and, moreover, the electronics for the step up process are relatively simple. The circuitry and operating characteristics of low voltage input, regulated, current drive DC-DC converters suitable for use with thermionic converters are described in References 2.5, 2.6 and 2.7.

Figure 2.2.4.1 shows representative efficiencies of current drive DC-DC converters for various voltage inputs and power levels. The data in Figure 2.2.4.1 indicates that there is little to be gained by using an input voltage greater than 5 volts, but that the efficiency falls off rapidly for input voltages less than 5 volts.

At a power level of 500 watts and an input voltage of 5 volts, a representative DC-DC converter efficiency of 89% is found from Figure 2.2.4.1. Thus, in order to obtain 500 watts of useful power it will be necessary to supply 560 watts to the DC-DC converter. Therefore the thermionic converters will be designed so that several connected in series



# REPRESENTATIVE DC-DC CONVERTER EFFICIENCIES

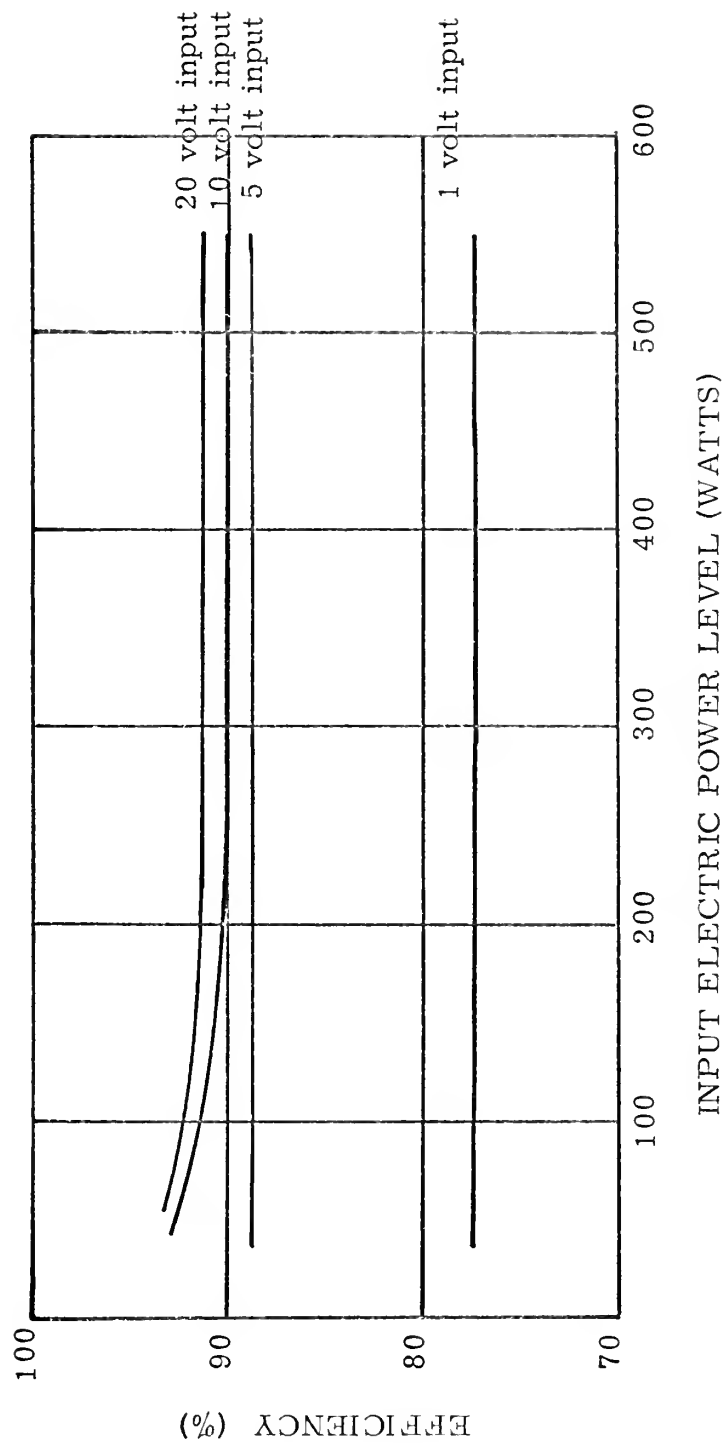


FIGURE 2.2.4.1





will provide 560 watts at 5 volts to a DC-DC converter.

Now that the thermionic converter output requirements have been established the power flattening problem must be investigated to determine whether or not it restricts the selection of the thermionic converter operating point.

## 2.3 THERMIONIC CONVERTER DESIGNS COMPATIBLE WITH POWER FLATTENING REQUIREMENTS

### 2.3.1 POWER FLATTENING REQUIREMENTS

Since the half life of cobalt-60 is 5.25 years, the energy supplied to the emitter heat source will decrease significantly over the three year life of the power supply. This means that some form of power flattening must be employed so that constant power can be supplied to the load.

Since a constant emitter operating temperature of  $2000^{\circ}\text{K}$  has been chosen for this design, the power flattening problem reduces to one of maintaining the emitter heat source at a constant temperature while the energy available from the cobalt-60 decreases. There are two general approaches to this power flattening problem. The first is to remove all the energy deposited in the emitter heat source through the thermionic converter. This approach necessitates operating with a variable cesium reservoir temperature. The second approach allows the thermionic converter to operate at a fixed power point (i. e. constant output voltage and current). In order to do this a variable heat removal system is connected to the emitter heat source and operates in parallel with the thermionic converters.

### 2.3.2 CONVERTER OPERATION WITH VARYING CESIUM RESERVOIR TEMPERATURE

When operating near maximum efficiency the major fraction of the



heat transferred from the emitter to the collector is carried by the electrons. If the emitter is maintained at a constant temperature the only other significant heat transfer, that due to radiation, remains constant. Thus, in order to vary the emitter cooling rate, the output current must be varied. Figure 2.2.1.1 shows that the output current can be varied by varying the cesium reservoir temperature.

In order to maintain a constant power output the output voltage would also have to be varied. As can be seen from Figures 2.2.1.2 and 2.2.1.3 the current density and power output are both functions of the converter output voltage and cesium reservoir temperature.

Over a three year period the energy released by the cobalt-60 decreases by 33%. This means that the current density would also have to vary by 33% and in order to maintain a constant power output the output voltage must also be varied by 33%. The DC-DC converters described in References 2.5 and 2.6 can accommodate a  $\pm 14\%$  variation in input voltage. Thus it would be desirable to employ a system that would decrease the variation in output voltage so that a more complex DC-DC converter does not have to be designed. It was therefore decided that the operation of a thermionic converter at a constant output voltage would be investigated.

In order to maintain a constant emitter temperature while operating at a constant output voltage, it is necessary to control both the cesium reservoir temperature and the voltage regulator shunt resistance. In the range of voltage outputs over which a variation in cesium reservoir temperature can cause a 33% variation in the current output density a decrease in the cesium reservoir temperature causes a decrease in output current density.

Therefore the thermionic converter would be designed to provide the



desired power level with a low cesium reservoir temperature at the end of life. In order to cool the emitter at a faster rate at the beginning of life, the converter would be operated at a higher cesium reservoir temperature and consequently a high current density. Since the output voltage is held constant, the power output will always be higher than required until the end of design lifetime is reached. This means that the thermionic converter would have to be coupled to the load with a dissipative shunt regulator (such as described in Reference 2.5) which would maintain a constant power output to the load.

Figures 2.2.1.2 and 2.2.1.3 show the intrinsic efficiency and output power density as functions of output voltage and cesium reservoir temperature. The data in these figures was used to predict the beginning of life performance of a thermionic converter designed to operate at a constant output voltage and variable cesium reservoir temperature.

Even though the emitter would be maintained at a constant temperature, the exponentially decreasing heat flux to the collector would cause its temperature to decrease because of the fixed heat transfer area of the collector radiation. Therefore Figures 2.2.1.4 and 2.2.1.5, which show intrinsic efficiency and output power density as a function of collector temperature and output voltage, were used to predict the end of life performance of the thermionic converter.

It was found that at output voltages higher than 0.7 volts variation of the cesium reservoir temperature could not cause enough change in the output power density to provide the desired three year lifetime and still maintain a reasonable efficiency. Thus 0.7 volts was selected as the operating output voltage for the individual thermionic converters. This means that seven thermionic converters would have to be connected in series to



provide a 4.9 volt input to the DC-DC converter. The beginning and end of life characteristics of the thermionic converter designed to operate at a constant output voltage and with variable cesium reservoir temperature are summarized in Table 2.3.2.1. The input power requirements listed in Table 2.3.2.1 were calculated using the intrinsic efficiency.

### 2.3.3 OPERATION AT A FIXED POWER POINT

In order to allow the thermionic converter to operate at a fixed power point, a system must be provided which maintains the emitter heat source at a constant temperature while the thermionic converter removes a constant amount of heat. The usual approach is to provide a heat removal system which operates in parallel with the thermionic converters. Some parameter of the heat removal system, such as heat transfer area, is varied such that the excess heat removed decreases with the same time constant as the exponential decay of the isotope fuel. Reference 2.7 gives an excellent review of some of the more promising methods of power flattening. Unfortunately the only concept discussed that is neither beyond the present state of the art nor too complex to be simply automated is one which employs a variable radiator area. This method provides only approximate power flattening since the radiating surface is reduced in finite steps by ejecting parts of the radiator. In order to provide for the 33% variation in the heat input to the emitter heat source and maintain it at a relatively constant temperature, the radiator would have to be made up of many segments and would be very cumbersome.

Thus none of these proposed power flattening schemes seem particularly well suited to this design's requirement of a three year lifetime. Therefore, a power flattening mechanism was designed to





# CHARACTERISTICS OF CONVERTER WITH VARIABLE CESIUM RESERVOIR TEMPERATURE

	Beginning of Life	End of Life
Emitter Material	Tungsten	-
Emitter Temperature ( $^{\circ}\text{K}$ )	2000	2000
Collector Material	Molybdenum	-
Collector Temperature ( $^{\circ}\text{K}$ )	1000	750
Interelectrode Spacing	7 mils	-
Output Voltage (Volts)	0.7	0.7
Output Power Density ( $\text{Watts}/\text{cm}^2$ )	17.4	10
Cesium Reservoir Temperature ( $^{\circ}\text{K}$ )	630	608
Total Emitter Area ( $\text{cm}^2$ )	56	56
Total Power Output (Watts)	975	560
Required Heat Input (Watts)	4820	3150
Intrinsic Efficiency (%)	20.2	17.8
Design Lifetime (Years)	3.2	-
Number of Converters Required	7	-

TABLE 2.3.2.1



maintain a constant emitter temperature. This mechanism is described in Chapter 5. This power flattening mechanism made the design of a thermionic converter operating at a constant power point feasible. This converter would operate with the characteristics listed in Table 2.3.3.1. The converter was also designed using the performance characteristics presented in Figures 2.2.1.2 and 2.2.1.3. Again, the input power requirements were calculated using the intrinsic efficiency.

A converter operating with this mode of power flattening has the following advantages over a converter using a variable cesium reservoir temperature (Table 2.3.2.1) for power flattening. Its 920 watt lower thermal power input requirement results in a saving of \$12,900 on initial fuel costs based on a cost of \$14 per thermal watt (Reference 1.2). Only five thermionic diodes are needed to provide the desired 5 volt input to the DC-DC converter instead of the seven required by the system using the variable cesium reservoir temperature mode of power flattening. Since the cesium reservoir temperature remains constant over the entire operating period, an internal adsorption type reservoir of the type described in Reference 2.9 can be used.

Since these advantages strongly favor a thermionic converter operating at a constant power point, a thermionic converter with the operating characteristics given in Table 2.3.3.1 was selected for use in this power supply design.



CHARACTERISTICS OF A CONVERTER OPERATING AT A  
CONSTANT POWER POINT

	Beginning of Life	End of Life
Emitter Material	Tungsten	-
Emitter Temperature ( $^{\circ}\text{K}$ )	2000	2000
Collector Material	Molybdenum	-
Collector Temperature ( $^{\circ}\text{K}$ )	1000	1000
Interelectrode Spacing	7 mils	-
Output Voltage (volts)	1.0	1.0
Output Power Density ( $\text{watts}/\text{cm}^2$ )	8.8	8.8
Cesium Reservoir Temperature ( $^{\circ}\text{K}$ )	610	610
Total Emitter Area ( $\text{cm}^2$ )	63.5	63.5
Total Power Output (watts)	560	560
Required Heat Input (watts)	2540	2540
Excess Fuel Required (watts)	1360	0
Intrinsic Efficiency (%)	22	22
Design Lifetime (Years)	3.2	-
Number of Converters Required	5	-

TABLE 2.3.3.1



## REFERENCES

- 2.1 Wilkins, D.R., "An Improved Theoretical Description of Thermionic Converter Performance Characteristics," Proceedings: 27th Annual Physical Electronics Conference, Cambridge, Mass., March, 1967.
- 2.2 Wilkins, D.R., "A Unified Theoretical Description of Thermionic Converter Performance Characteristics," Journal of Applied Physics, vol. 39, number 5, April, 1968.
- 2.3 Paquin, M.L., "High Temperature Multi-Foil Thermal Insulation," Thermo Electron Corp.
- 2.4 Corliss, W.R. and Harvey, D.G., Radioisotopic Power Generation, Englewood Cliffs: Prentice Hall, Inc., 1964.
- 2.5 Lingle, J.T., "Thermionic Low Voltage Converter Regulator Systems," Conference Record of the Thermionic Conversion Specialist Conference, November, 1966.
- 2.6 Lingle, J.T., "Low Input Voltage Conversion," Proceedings of the 18th Annual Power Sources Conference, May, 1964.
- 2.7 Lingle, J.T., "Energy Source - Low Voltage Conversion System," Proceedings of the 19th Annual Power Sources Conference, 1965.
- 2.8 Rush, R.E. and Belofsky, H., "Power Flattening Studies for Radioisotope Thermoelectric Generators," General Instruments Corp., NYO-9783, 1963.
- 2.9 Harbaugh, W.E. and Basiulis, A., "The Development of a High-Temperature Reservoir for Automatic Control of Cesium Pressure," Conference Record of the Thermionic Conversion Specialist Conference, November, 1966.





## CHAPTER 3

### FUEL ELEMENT OPTIMIZATION

#### 3.1 GENERAL REMARKS

This chapter explains in detail the methods used to optimize the the fuel element design. Limitations placed on the fuel element geometry are discussed and two practical fuel element configurations, which were selected for study, are described.

The heat losses which contribute to fuel element inefficiencies are defined and the methods used to calculate these heat losses are explained in detail. Heat losses and efficiencies, calculated for fuel elements of various lengths, diameters and strengths, are compared. Based on this comparison the optimum fuel element design is selected for use in this power supply design.

#### 3.2 FUEL ELEMENT CONFIGURATION

The major supplier of cobalt-60 is the Atomic Energy Commission's Savannah River Laboratory. The cobalt is obtainable in the form of wafers which are 40 mils thick and up to 3.5 inches in diameter. Each wafer is plated with approximately one mil of nickel in order to prevent contamination of the equipment used to handle it once it has been irradiated. (Reference 3.1) Due to the size limitations placed on the cobalt wafers any fuel element large enough to be of interest will have to be composed of a large number of wafers.

The two fuel element configurations which were considered for this power supply design are shown in Figures 3.2.1 and 3.2.2. One fuel element is composed of a stack of cobalt wafers which form a solid cylinder; the other is composed of washer like cobalt wafers and takes a



## CROSS SECTION OF SOLID FUEL ELEMENT

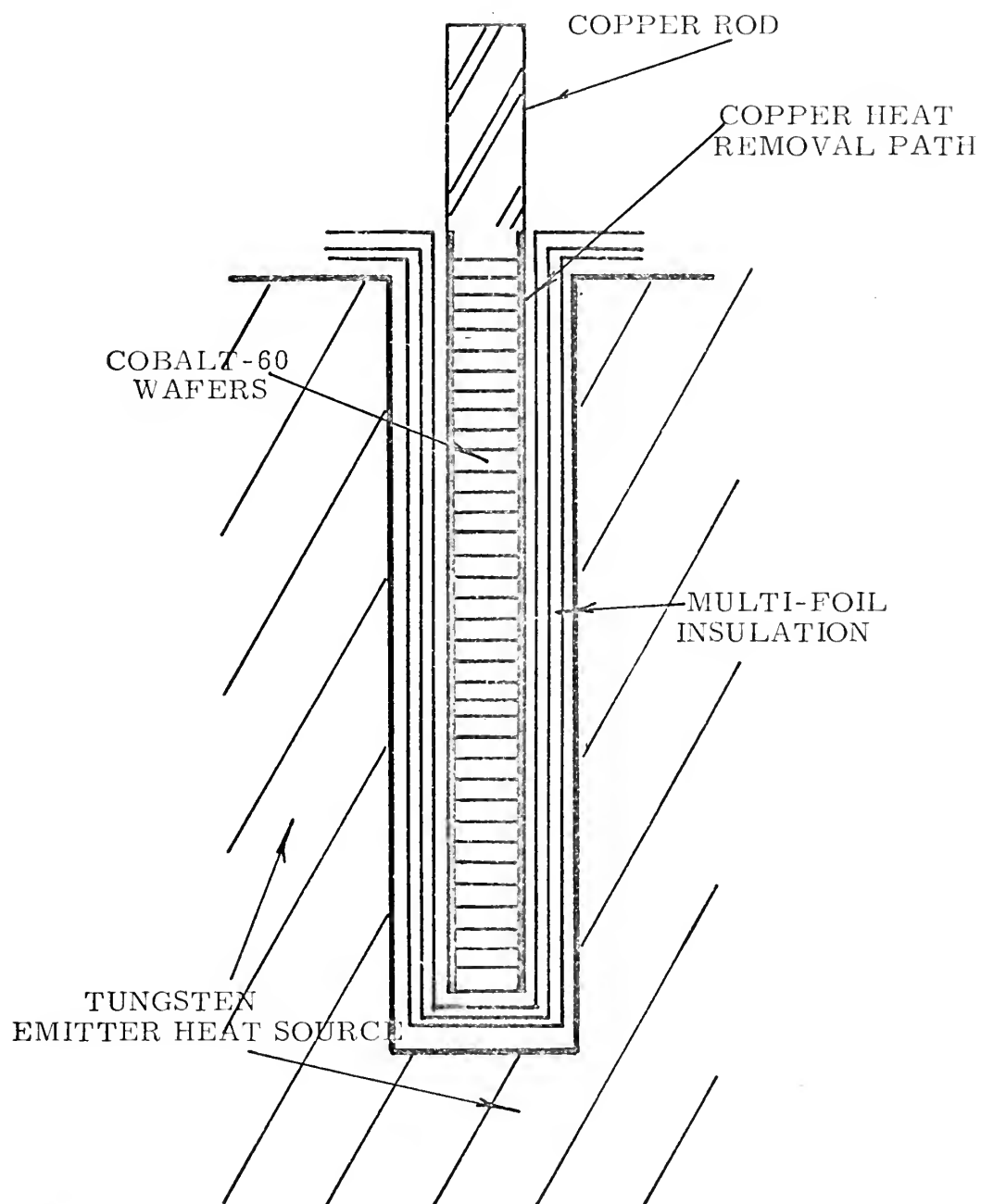


FIGURE 3.2.1



## CROSS SECTION OF TUBULAR FUEL ELEMENT

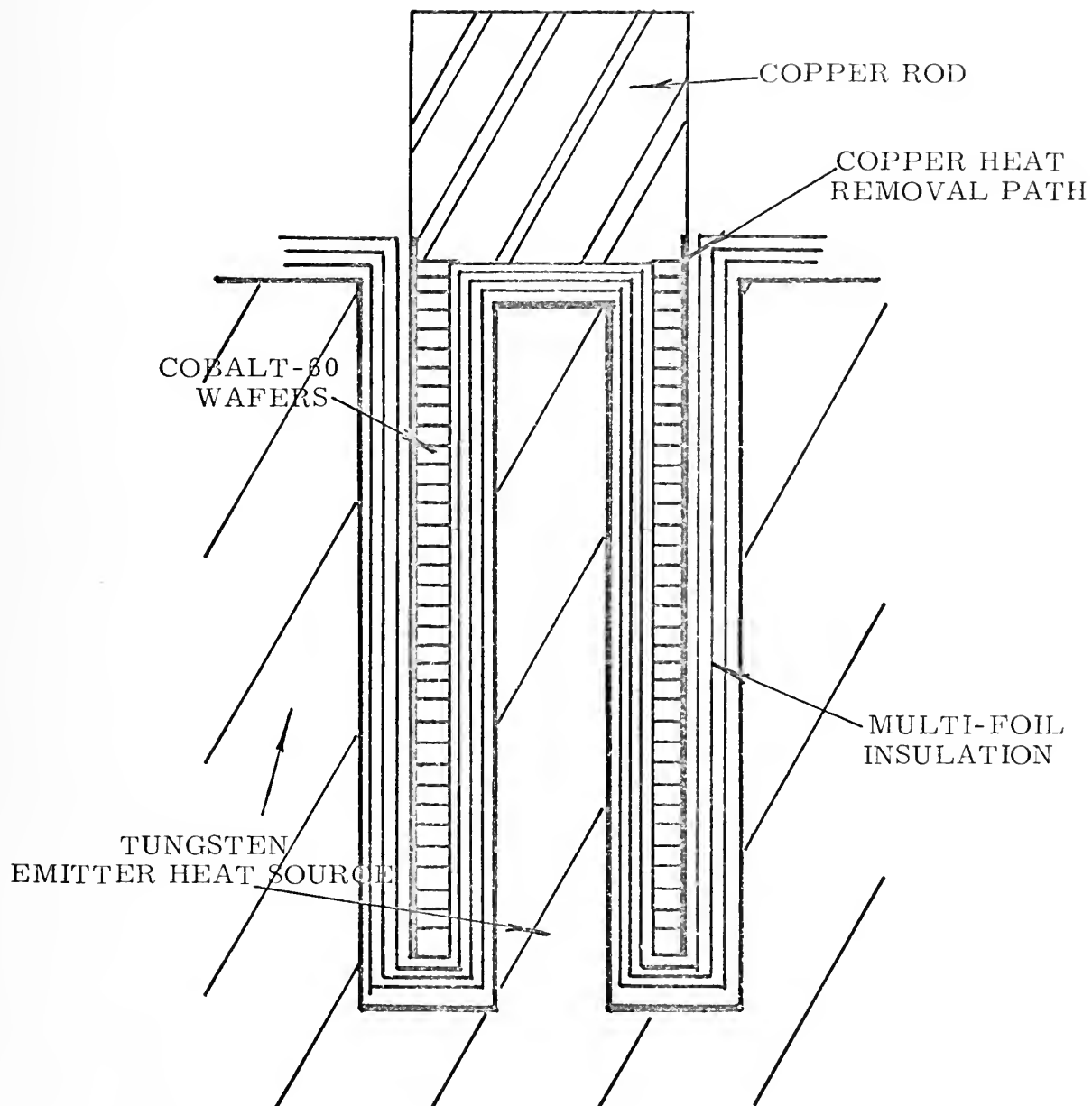


FIGURE 3.2.2



tubular form. The fuel elements are both clad in copper. They are insulated from the emitter heat source with multi-foil insulation and are designed to operate at low temperatures.

In order to insure that the fuel is maintained at a low temperature any heat generated in it due to the self absorption of gamma radiation or any heat which reaches it through the thermal insulation must be removed. When stacked to form a fuel element, the cobalt wafers offer a very poor heat transfer path due to the low thermal conductance across the wafer interfaces. Thus the fuel element design must provide a means of removing any heat generated in the fuel element. In this case the stack of fuel wafers is clad in copper which provides a path of high thermal conductance for heat removal.

For future reference the fuel element is defined as the cobalt wafers, the copper heat removal path (cladding) and the surrounding multi-foil insulation. The cobalt wafers and copper cladding will be referred to as the fuel rod.

Since the fuel element is thermally insulated from the emitter heat source it is obvious that any energy which is absorbed in the fuel or any heat which is transmitted through the insulation to the fuel can not be used by the thermionic converter. It will therefore be beneficial to design the fuel element so that the total energy which the system loses to it will be minimized.

### 3.3 ENERGY LOSSES TO THE FUEL ELEMENTS

In order to minimize the total energy loss to the fuel elements it is necessary to know what the losses are and how to calculate them. Thus, the energy loss rates are defined in this section. The methods used to calculate them are then explained in the following sections.





$E_{\beta} \equiv$  energy loss due to absorption of beta particles in the cobalt and copper per unit time.

$E_{\gamma F} \equiv$  energy loss due to self absorption of gamma radiation in the cobalt per unit time.

$E_{\gamma C} \equiv$  energy loss due to absorption of gamma radiation in the copper heat removal path per unit time.

$E_{\gamma I} \equiv$  energy loss due to absorption of gamma radiation in the insulation per unit time.

$E_{\gamma S} \equiv$  energy loss due to the absorption of backscattered gamma radiation in the fuel element per unit time.

$Q_I \equiv$  energy loss due to heat flux through the insulation from the tungsten to the fuel element.

### 3.4 FUEL ELEMENT EFFICIENCY

The efficiency of the fuel element,  $\eta_F$ , is defined as

$$\eta_F = 1 - \frac{(E_F + E_C + E_I + E_S + Q_I + E_{\beta})}{E_T} \quad (3.4.1)$$

where  $E_T$  is defined as the total energy released during radioactive decay of the fuel per unit time minus any energy carried away by neutrinos.

This definition is compatible with the convention used when calculating the power density of the fuel.

### 3.5 CALCULATION OF $E_{\beta}$

$E_{\beta}$  is the simplest energy loss to calculate. The beta particles resulting from the decay of the cobalt-60 are emitted with an energy spectrum which has an upper energy limit of 0.31 Mev. The range of the most energetic beta particle is 81 mg/cm<sup>2</sup> which is equivalent to 0.009 cm of cobalt. Since this distance is much shorter than any fuel chord length all of the beta energy is absorbed in the fuel. This means that 0.31 Mev are lost to the system for each disintegration of a cobalt-60 atom. However, 71% of this beta decay energy is carried away by neutrinos (Reference 3.2);



thus only 0.09 Mev's per disintegration are deposited in the fuel.

A sample of cobalt-60 with an activity of 400 curies per gram will release a total of 58.7 watts/cm<sup>3</sup>; 52.4 watts/cm<sup>3</sup> is in the form of gamma radiation, 4.4 watts/cm<sup>3</sup> is carried away by the neutrinos and 1.9 watts/cm<sup>3</sup> appears as beta particle energy. Thus

$$E_{\beta} = 1.9 V_F \quad (3.5.1)$$

where  $V_F$  is the volume of the fuel (cobalt-60) in cm<sup>3</sup>. Equation 3.5.1 is valid only for cobalt with an activity of 400 curies per gram.

### 3.6 CALCULATION OF $E_{\gamma F}$

In order to calculate  $E_{\gamma F}$ , the results of calculations performed and described in detail in Reference 3.3 were used. This reference treats the finite source as a series of planes composed of point isotropic sources and integrates over the volume assuming scattering is straight ahead and attenuation is exponential. This integral can be performed analytically only if planes and cylinders of infinite length are considered. The results obtained are plotted in Figure 3.6.1 as a self absorption factor,  $f$ , which is equal to the fraction of emitted gamma radiation absorbed in the fuel.

Thus,

$$E_{\gamma F} = f (E_T - E_{\beta}) \quad (3.6.1)$$

### 3.7 CALCULATION OF $E_{\gamma C}$ AND $E_{\gamma I}$

$E_{\gamma C}$  and  $E_{\gamma I}$  were computed using the following method developed in Reference 3.3.  $I_p$  is defined as the intensity of absorbed radiation per unit volume per second at a distance  $r$  from the axis of a cylinder and in a plane coincident with the end of the cylinder.



# GAMMA SELF ABSORPTION FACTOR

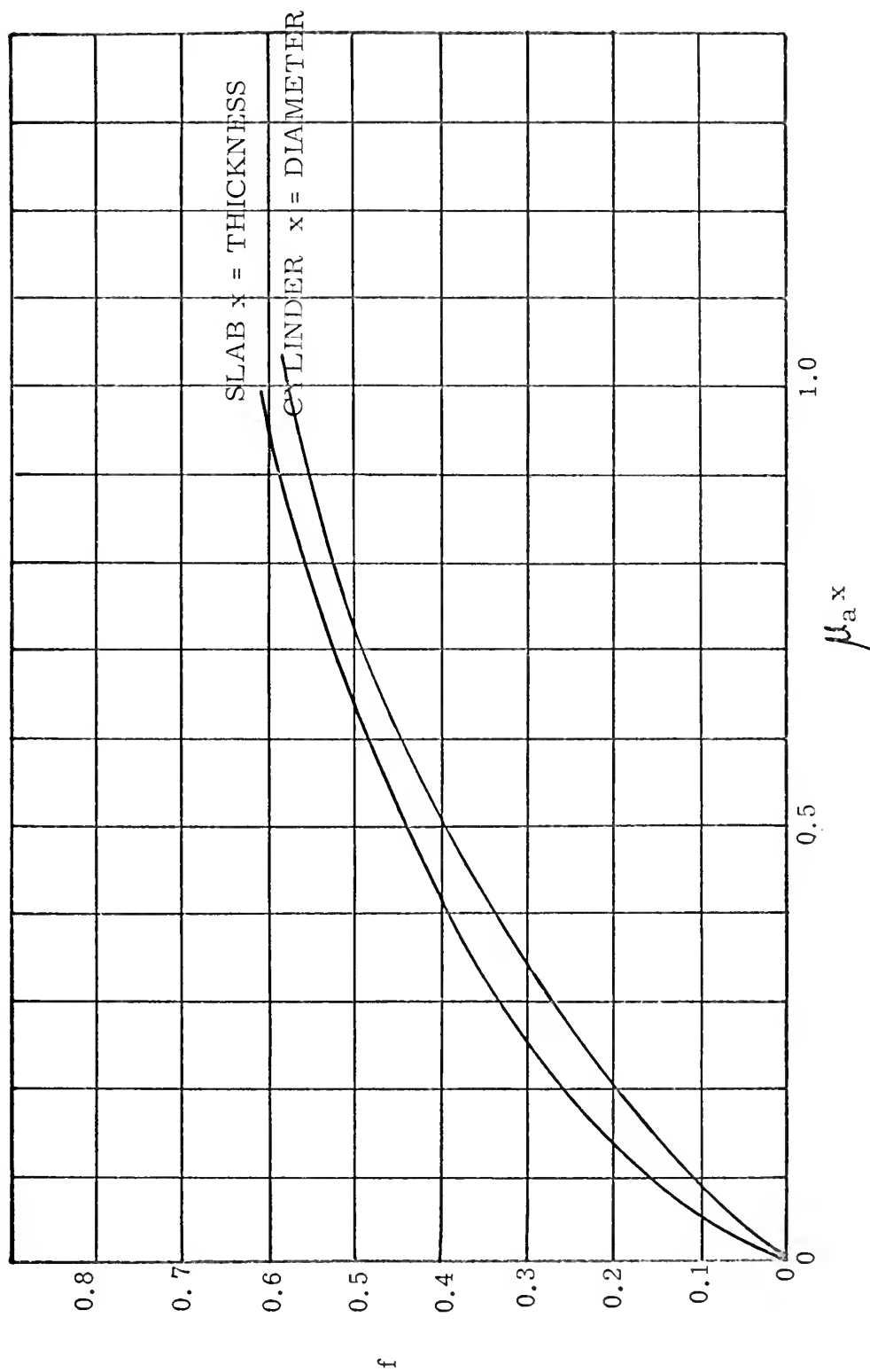


FIGURE 3.6.1



$$I_p = \int_0^\infty dz \int_0^{2\pi} d\Theta \int_0^R \frac{\mu_a e^{-\mu_a D}}{4\pi D^2} \rho \, d\rho \quad (3.7.1)$$

where  $\mu_a$  is the macroscopic gamma absorption cross section of the material surrounding the fuel at the energy of the emitted gamma radiation and  $D$  is related to  $\rho$ ,  $\Theta$  and  $z$  by

$$D^2 = z^2 + \rho^2 + r^2 - 2r\rho \cos \Theta \quad (3.7.2)$$

See Figure 3.7.1.

The value of  $I_p$  obtained from equation 3.7.1 is one half the value of the radial distribution in any normal plane of an infinite cylinder. Therefore, a new function  $I_p'$  is defined where

$$I_p' = \frac{2I_p}{1 - f} \quad (3.7.3)$$

$I_p'$  is the normalized absorbed radiation intensity so that

$$\int_0^\infty \frac{2I_p'}{\mu_a R} r' \, d[\mu_a R(r' - 1)] = 1 \quad (3.7.4)$$

where  $R$  is the radius of the fuel and  $r'$  is equal to  $r/R$ .

The function  $\left[ \frac{2I_p'}{\mu_a R} \right] r'$  is plotted against  $\mu_a R(r' - 1)$  in Figure 3.7.2.

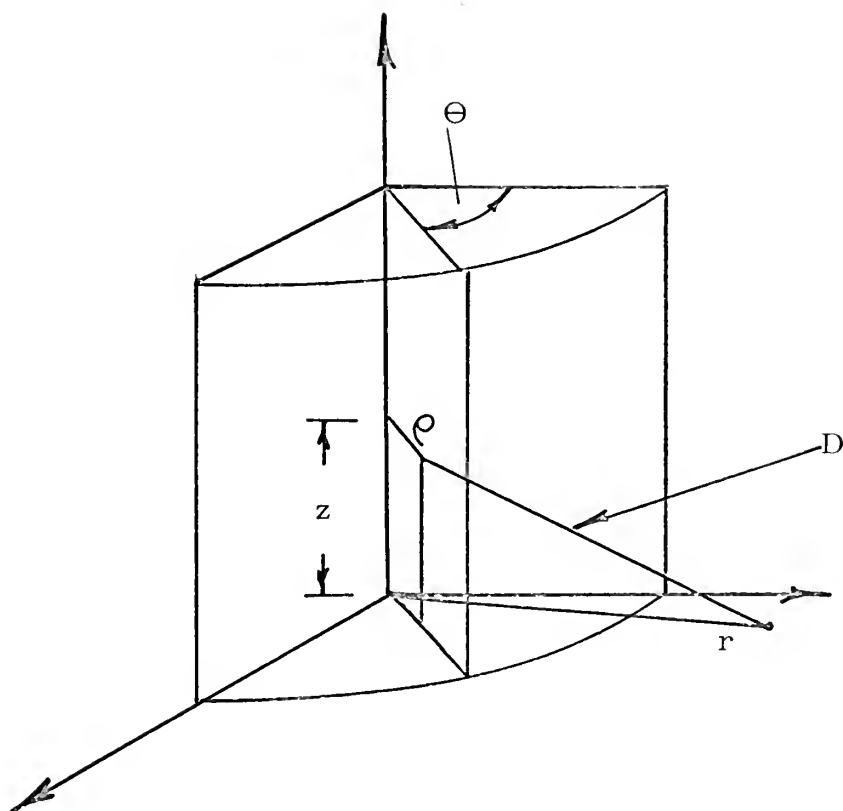
The fraction of the emerging energy that is absorbed in an annular shell between  $r_1$  and  $r_2$  is equal to

$$\int \frac{\mu_a (r_2 - R)}{\mu_a (r_1 - R)} \frac{2I_p'}{\mu_a R} r' \, d[\mu_a R(r' - 1)] \quad (3.7.5)$$

This integration can be performed graphically on Figure 3.7.2.







GEOMETRY USED IN THE CALCULATION OF  $I_p$

FIGURE 3.7.1



# NORMALIZED INTENSITY OF ABSORBED RADIATION

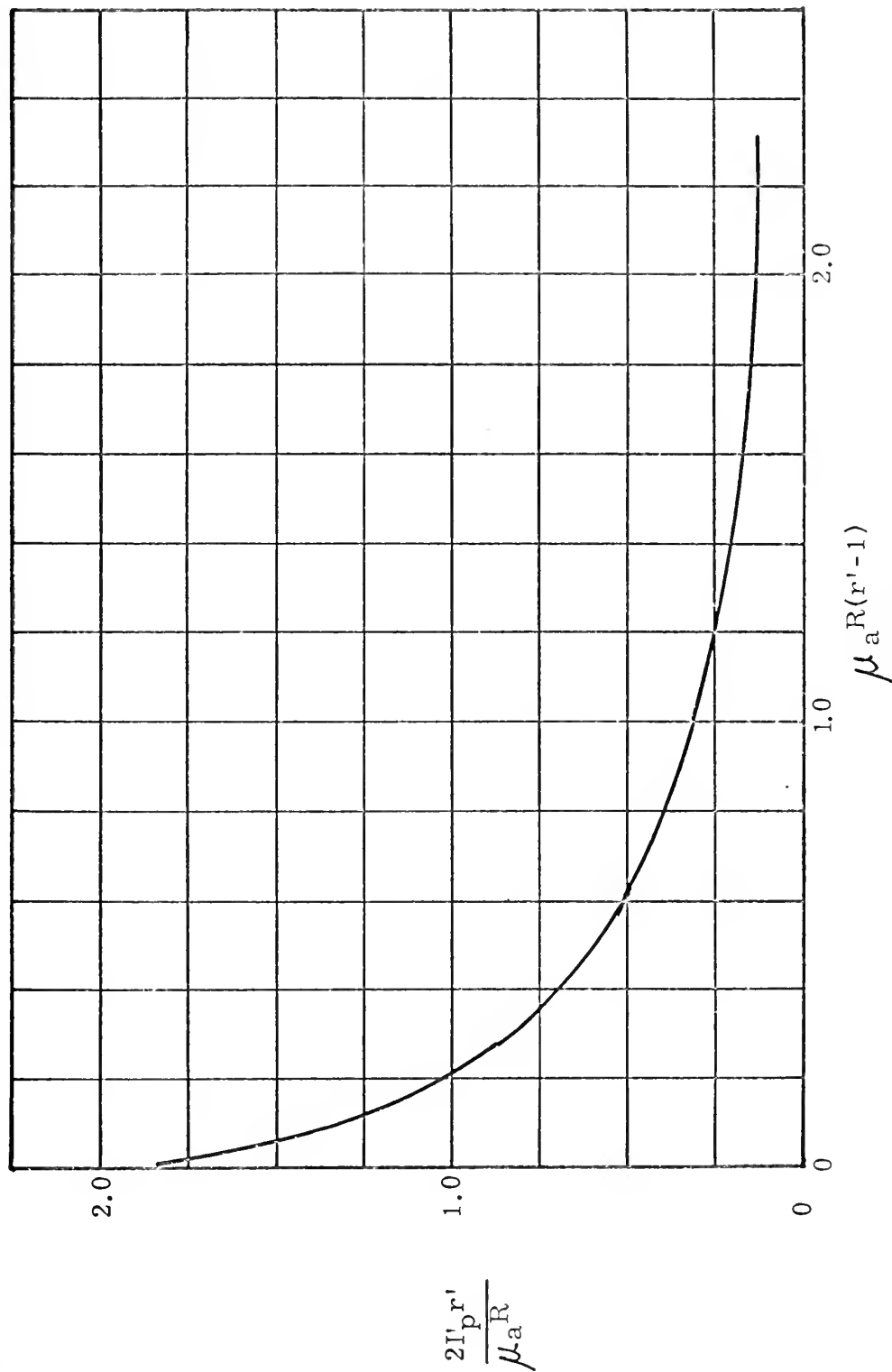


FIGURE 3.7.2



$E_{\gamma C}$  is equal to

$$(E_T - E_{\beta} - E_{\gamma F}) \int_0^{\mu_a(r_C - R)} \frac{2I_p'}{\mu_a R} r' d[\mu_a R(r' - 1)] \quad (3.7.6)$$

where  $r_C$  is the outer radius of the copper.  $E_{\gamma I}$  is equal to

$$(E_T - E_{\beta} - E_{\gamma F}) \int_{\mu_a(r_C - R)}^{\mu_a(r_I - R)} \frac{2I_p'}{\mu_a R} r' d[\mu_a R(r' - 1)] \quad (3.7.7)$$

where  $r_I$  is the equivalent outer radius of the multi-foil insulation. The equivalent radius is defined such that  $r_I - r_C$  is equal to the sum of the thicknesses of the individual foils in the insulation.

### 3.8 CALCULATION OF $E_{S\gamma}$

$E_{S\gamma}$  was approximated in the following manner. The number and energy albedo for tungsten for gamma radiation as a function of energy are shown in Figure 3.8.1. These curves were found by interpolating the data found in Reference 3.4.

The average energy of the backscattered radiation  $E_S$  is defined as

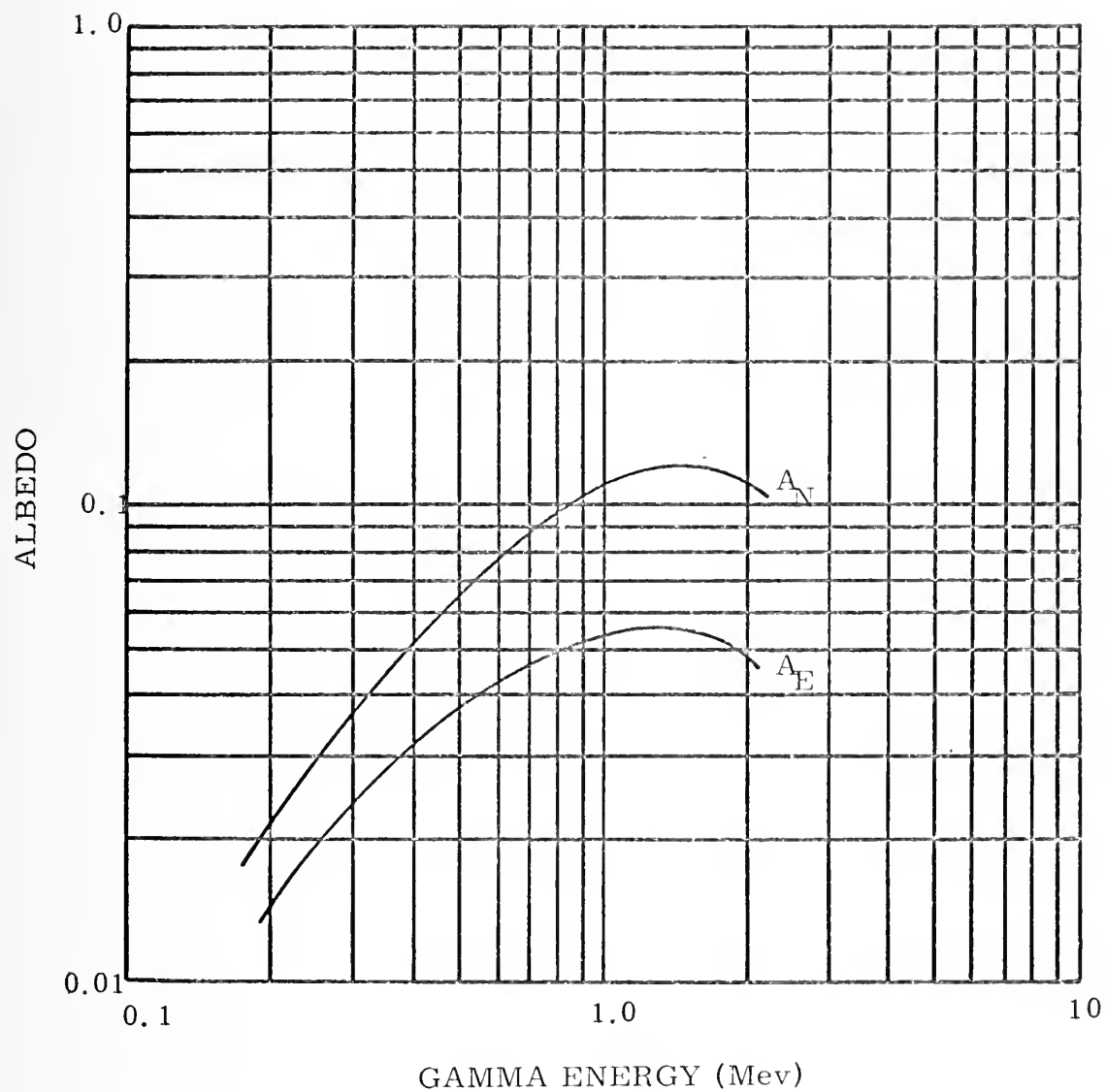
$$E_S \equiv \frac{E_I \times A_E}{A_N} \quad (3.8.1)$$

where  $E_I$  is the initial energy of the gamma radiation,  $A_E$  is the energy albedo at  $E_I$  and  $A_N$  is the number albedo at  $E_I$ .

Once the value of  $E_S$  is obtained the energy absorption cross section of the fuel  $\mu_{aF}$  is evaluated at this average energy.

The backscattered radiation is assumed to constitute a planar isotropic source at the surface of the fuel rod. The average distance that





ISOTROPIC SOURCE GAMMA ALBEDO FOR TUNGSTEN

FIGURE 3.8.1





the backscattered radiation travels through the fuel rod is equal to the mean chord length of the fuel rod  $\bar{r}$ .

$$\bar{r} = \frac{4 \times \text{fuel rod volume}}{\text{fuel rod surface area}} \quad (3.8.2)$$

Thus

$$E_{S\gamma} = (E_T - E_{\beta} - E_{\gamma F} - E_{\gamma C}) [1 - \exp(-\mu_{aF} \bar{r})] \quad (3.8.3)$$

### 3.9 CALCULATION OF $Q_I$

The insulation selected for use in this design is composed of tungsten foils 0.5 mils thick and separated by thorium oxide. The average spacing per layer  $d$ , is 4.0 mils. Multi-foil of this composition has given satisfactory performance at 1900° C. (Reference 3.5)

Two terms contribute to the heat lost through the insulation,  $Q_I$ . One is the heat lost due to conduction through the insulation and the other is the edge loss. The latter arises from the difficulty of matching the foil layers at corners. The mismatching of the foil edges degrades the performance of the insulation. Data from Reference 3.6 indicates that the heat loss in watts per cm of edge is approximately twice the heat flux in watts per cm<sup>2</sup> through the insulation.

Figure 3.9.1 shows the thermal conductivity  $k_I$  of the multi-foil insulation as a function of source temperature.

$$Q_I = \frac{A k_I (T_S - T_F) + 2 L k_I (T_S - T_F)}{N d} \quad (3.9.1)$$

where  $A$  is the total insulated surface area,  $L$  is the total insulated edge length,  $N$  is the number of layers of foil,  $d$  is the average spacing per layer,  $T_S$  is the temperature of the emitter heat source and  $T_F$  is the fuel rod temperature. The foil thermal conductivity is evaluated at  $T_S$ .



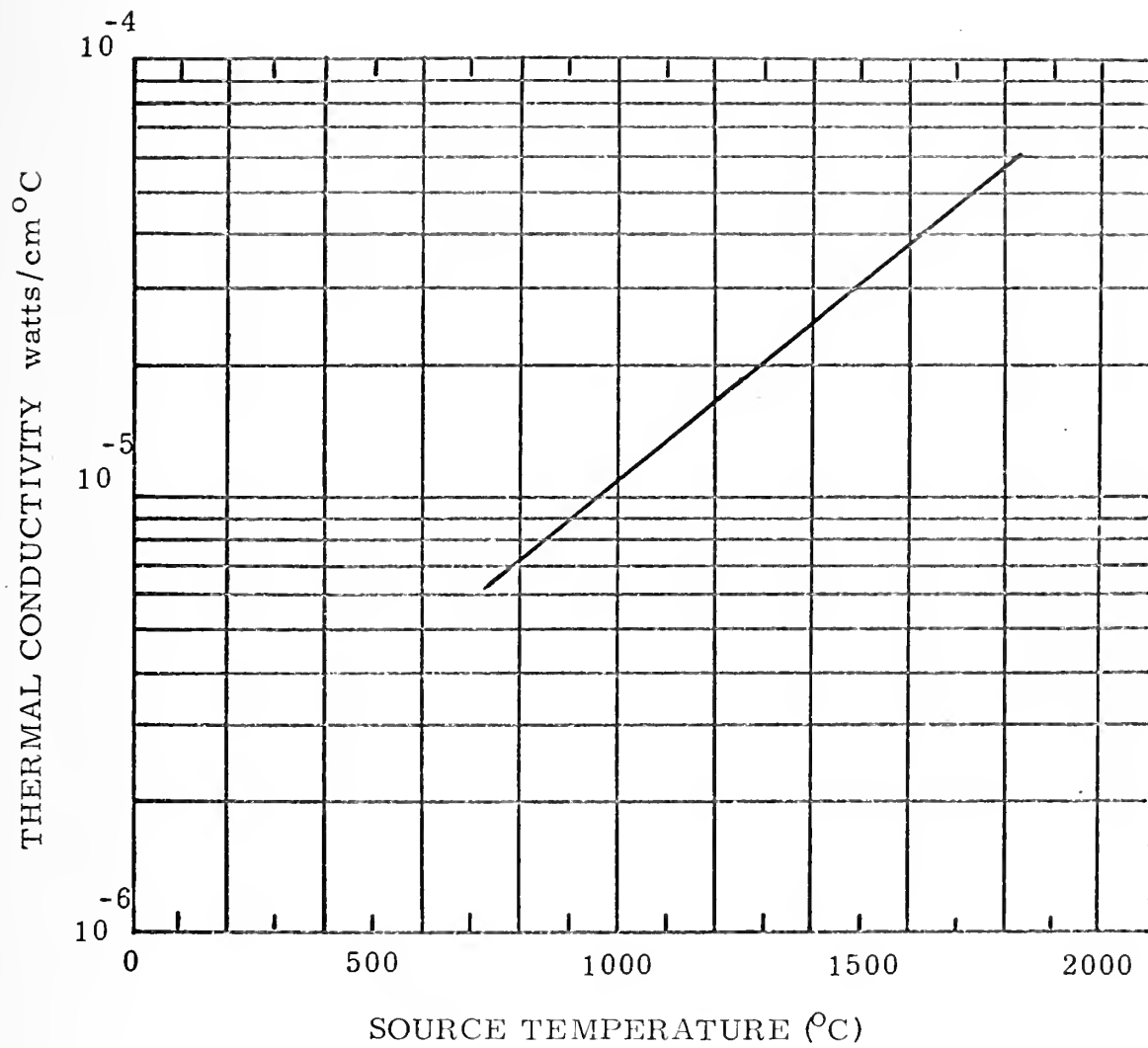
W-ThO<sub>2</sub> MULTI-FOIL INSULATION THERMAL CONDUCTIVITY ( $k_I$ )

FIGURE 3.9.1



### 3.10 EVALUATION OF SPECIFIC FUEL ELEMENTS

Once all the energy losses could be evaluated, the fuel elements were compared as follows. The fuel element configuration, strength and length were selected. The selected fuel element was then optimized and its efficiency calculated. The efficiencies were then compared in order to determine the optimum fuel element design.

Each fuel element evaluated was optimized in the following way. Values were selected for  $E_T$  and fuel element length. Then  $E_\beta$ ,  $E_{\gamma_F}$ ,  $E_{\gamma_I}$  and  $Q_I$  were calculated. The number of layers of insulation was selected so that the sum of  $E_{\gamma_I}$  and  $Q_I$  was a minimum. It was then assumed that heat equal to the sum of  $E_\beta$ ,  $E_{\gamma_F}$ ,  $E_{\gamma_I}$  and  $Q_I$  was generated uniformly in the copper heat removal path. This is a good assumption since the copper is very thin and has a high thermal conductivity. The temperature rise along the length of the fuel element was limited to  $300^\circ\text{C}$  and the outer radius,  $r$ , of the copper was calculated using Equation 3.10.1.

$$r^2 = \frac{(E_\beta + E_{\gamma_F} + E_{\gamma_I} + Q_I) L}{\Delta t \ 2\pi k_C} + R^2 \quad (3.10.1)$$

where  $\Delta t = 300^\circ\text{C}$ ,  $k_C$  is the thermal conductivity of copper,  $L$  is the length of the fuel element and  $R$  is the radius of the cobalt fuel. Once the thickness of the copper was determined,  $E_{\gamma_C}$  and  $E_{S\gamma}$  were calculated. Equation 3.4.1 was then used to calculate  $\eta_F$ .

In Figure 3.10.1,  $\eta_F$  is plotted against fuel element length for various values of  $E_T$  and a solid cylinder fuel element geometry. The monotonic increase in efficiency with decreasing  $E_T$  is due almost entirely to the decrease in self absorption. The decrease in self absorption is due to the decrease in the diameter of the fuel rods as  $E_T$  decreases.



## COMPARISON OF SOLID FUEL ELEMENT EFFICIENCIES

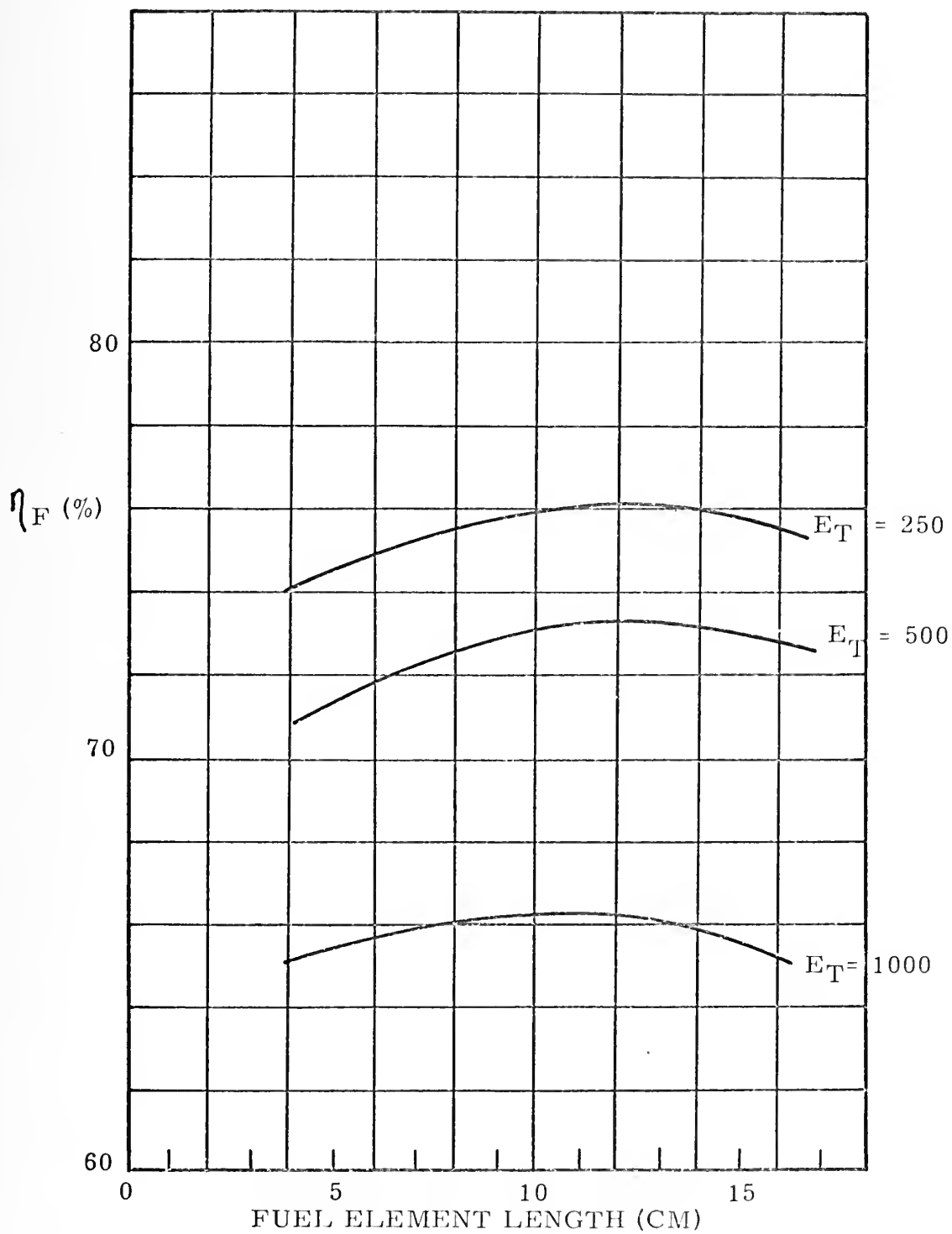


FIGURE 3.10.1





In Figure 3.10.2,  $\eta_F$  is plotted against fuel element length for  $E_T = 1000$  watts, but for the solid cylinder and tubular fuel element geometries. The higher efficiency of the tubular fuel element is due to a decrease in  $E_{\delta F}$  and  $E_{\delta C}$ . The gain in efficiency would be higher were it not for a significant increase in  $E_{\delta I}$  and  $Q_I$  for the tubular fuel element compared to the equivalent solid fuel element. See Table 3.10.2 for a tabulation of the various energy losses in these two fuel elements.

Figure 3.10.3 shows  $\eta_F$  as a function of fuel element diameter for a tubular fuel element with  $E_T = 1000$ . The efficiency increases with diameter up to 4 cm, then remains relatively constant and then decreases as the diameter becomes very large. The reasons for this behavior can best be seen from Table 3.10.3.  $E_{\delta F}$  decreases with increasing diameter since the cobalt becomes thinner.  $E_{\delta C}$  decreases with increasing diameter since the copper heat removal path can be made thinner. The decrease in  $E_{\delta F}$  and  $E_{\delta C}$  lead to an increase in efficiency. However, as can be seen from Table 3.10.3, the increasing surface area leads to a marked increase in  $Q_I$  which eventually overrides the decrease in  $E_{\delta F}$  and  $E_{\delta C}$  and causes the efficiency to decrease.

Table 3.10.1 shows the relative importance of the various components of the total heat loss and how they vary as the fuel element length is varied and  $E_T$  held constant at 1000 watts. Since the temperature drop along the fuel rod is held at  $300^\circ\text{C}$ , the thickness of the copper cladding must be increased as the fuel element length is increased. The increased copper thickness leads to an increase in  $E_{\delta C}$  which practically offsets the decrease in  $E_{\delta F}$ ; thus there is little variation in fuel element efficiency with length.

Based on the data presented in Figures 3.10.1 through 3.10.3 and



## COMPONENTS OF HEAT LOSS IN SOLID CYLINDER FUEL ELEMENTS

LENGTH	5 cm	10 cm	15 cm
$E_T$	1000	1000	1000
$E_\beta$	35	35	35
$E_{\gamma_F}$	222	174	145
$E_{\gamma_C}$	27	58.5	94.5
$E_{\gamma_I}$	18.5	21.2	26.4
$E_{S\gamma}$	17	14.1	14.3
$Q_I$	25.3	26.6	27.4
$\eta_F$	65.5 %	66.2 %	65.7 %

(ALL HEAT LOSSES IN WATTS)

TABLE 3.10.1



# COMPONENTS OF HEAT LOSS FOR DIFFERENT FUEL ELEMENT CONFIGURATIONS

## FUEL ELEMENT CONFIGURATION

	SOLID CYLINDER	TUBULAR
LENGTH	10 cm	10 cm
DIAMETER		4 cm
$E_T$	1000	1000
$E_\beta$	35	35
$E_{\delta_F}$	174	67.5
$E_{\delta_C}$	58.5	26.2
$E_{\delta_I}$	21.2	48
$E_{S\delta}$	14.1	5.2
$Q_I$	26.6	62.1
$\eta_F$	66.2 %	75.6 %

(ALL LOSSES IN WATTS)

TABLE 3.10.2



## COMPONENTS OF HEAT LOSS IN TUBULAR FUEL ELEMENTS

$E_T$	1000	1000	1000
DIAMETER	2 cm	4 cm	6 cm
$E_\beta$	35	35	35
$E_{\delta F}$	125	67.5	48.2
$E_{\delta C}$	50.5	26.2	18.3
$E_{\delta I}$	37.4	48	53.6
$E_{S\delta}$	9.4	5.2	3.4
$Q_I$	34.7	62.1	86.6
$\eta_F$	70.7 %	75.6 %	75.5 %

TABLE 3.10.3





COMPARISON OF  
SOLID AND TUBULAR FUEL ELEMENT EFFICIENCIES  
( $E_T = 1000$ )

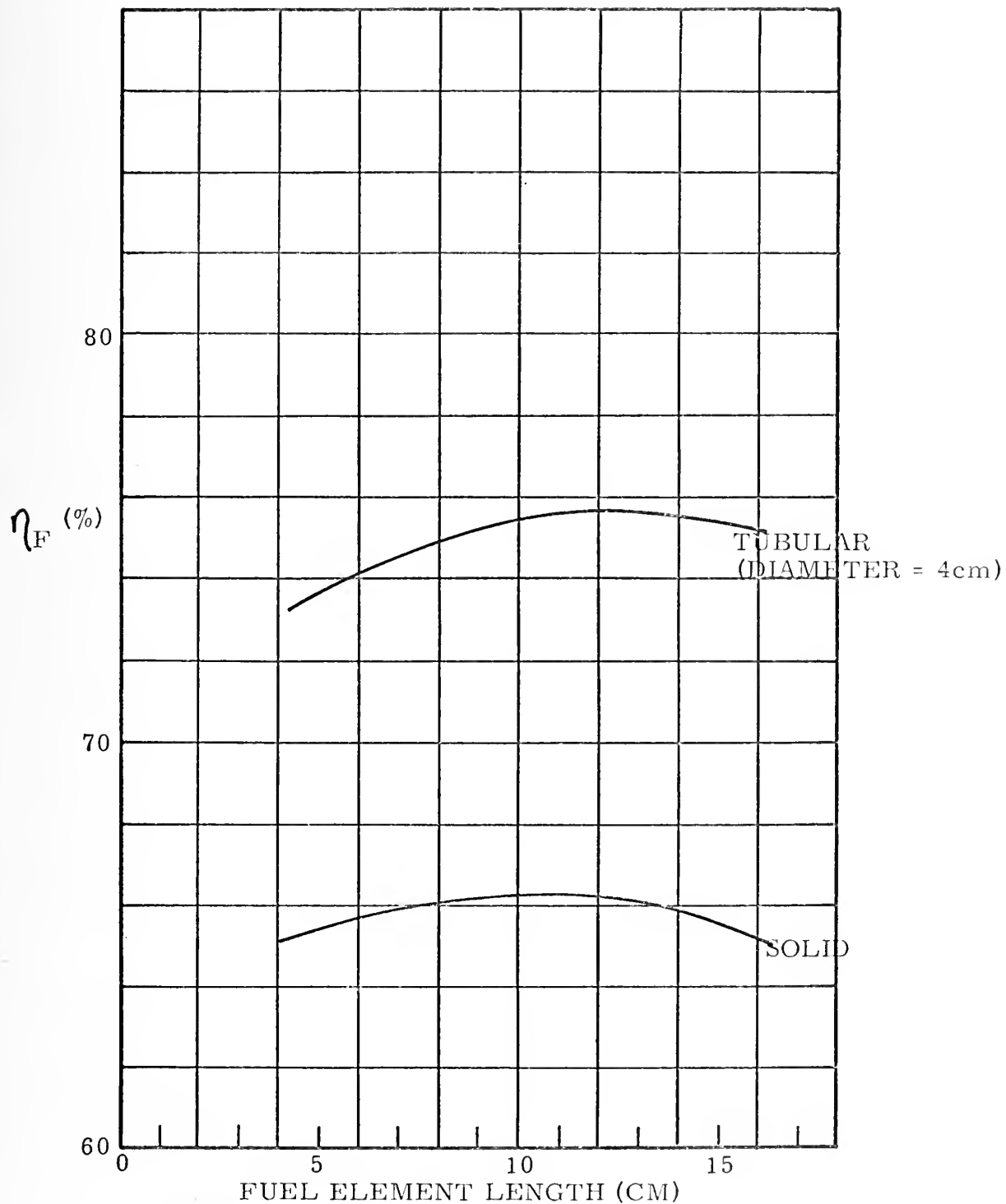


FIGURE 3.10.2



TUBULAR FUEL ELEMENT EFFICIENCY  
(LENGTH = 10 CM)

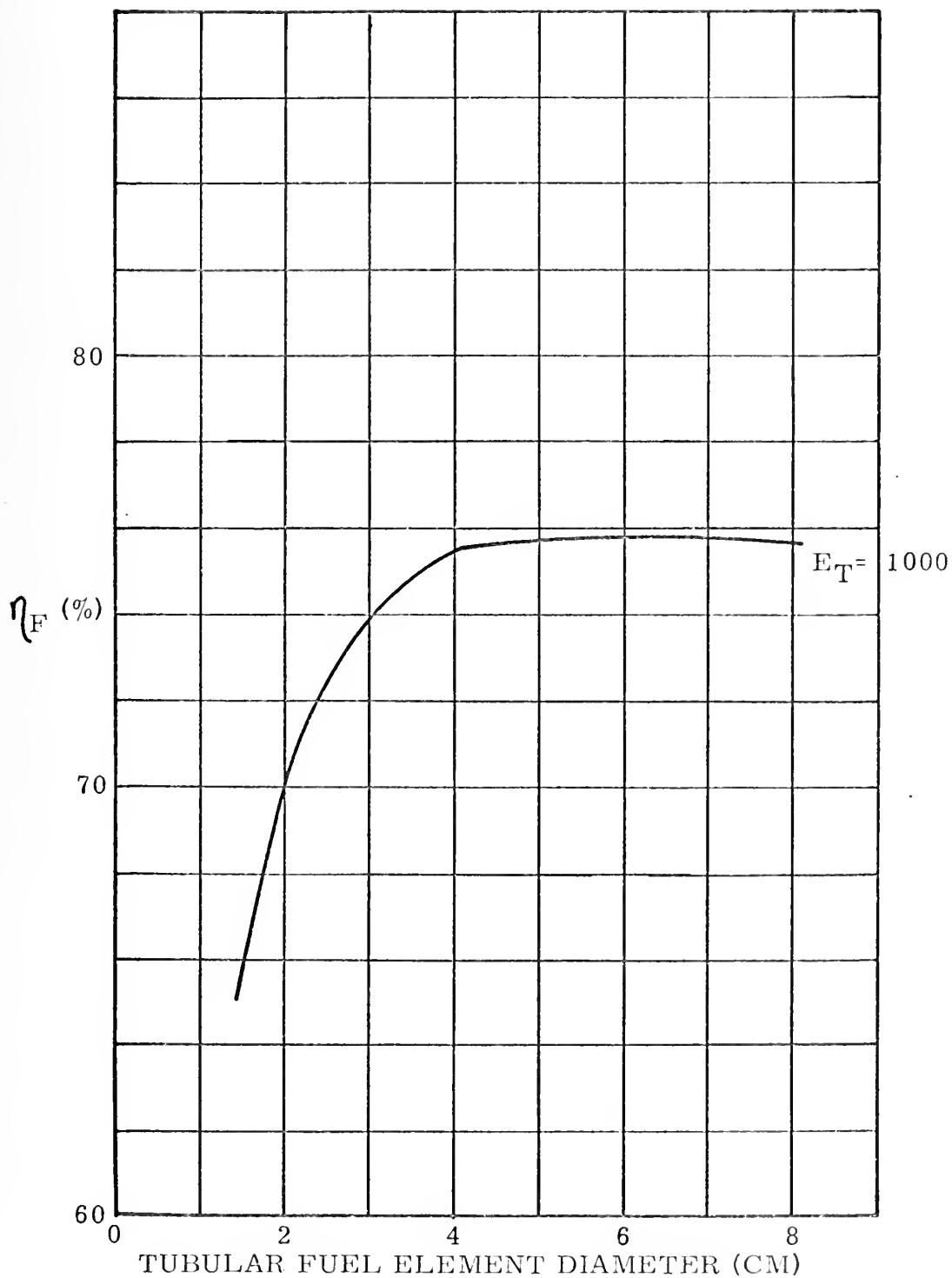


FIGURE 3.10.3



the power requirements listed in Table 2.3.3.1, it was decided that five tubular fuel elements would be used, each 4 cm in diameter, 10 cm long and with an  $E_T$  of 1000 watts.



## REFERENCES

- 3.1 Farace, J. P., "Experimental Cobalt-60 Heat Source Capsules," Savannah River Laboratory, DP-1145.
- 3.2 Corliss, W.R. and Harvey, D.G., Radioisotopic Power Generation, Englewood Cliffs: Prentice Hall, Inc., 1964.
- 3.3 Storm, M. L., Hurwitz Jr., H., and Roe, G. M., "Gamma Ray Absorption Distributions for Plane, Spherical and Cylindrical Geometries," General Electric Company, Knolls Atomic Power Laboratory, KAPL-783.
- 3.4 Berger, M. J. and Raso, D. J., "Monte Carlo Calculations of Gamma Ray Backscattering," Radiation Research 12, 20-37, 1960.
- 3.5 Paquin, M. L., "High Temperature Multi-Foil Thermal Insulation," Thermo Electron Corp.
- 3.6 Carvalho, J. and Dunlay, J. B., "Quarterly Progress Report of Research and Development of Vacuum Foil-Type Insulation for Radioisotope Power Systems," Thermo Electron Corp., TE Report No. 4059-109-69, January 20, 1969.





## CHAPTER 4

### SHIELDING

#### 4.1 GENERAL REMARKS

Radiosotope fueled generators intended for terrestrial use generally require considerable shielding since personnel may inadvertently come in contact with them even though they may be installed in remote locations. The Interstate Commerce Commission's shipping regulations for radioactive materials were therefore selected as the design criteria which the shielding for this power supply must satisfy. These regulations specify a maximum dose rate of 200 mr/hr at the shield surface and 10 mr/hr one meter from the shield surface.

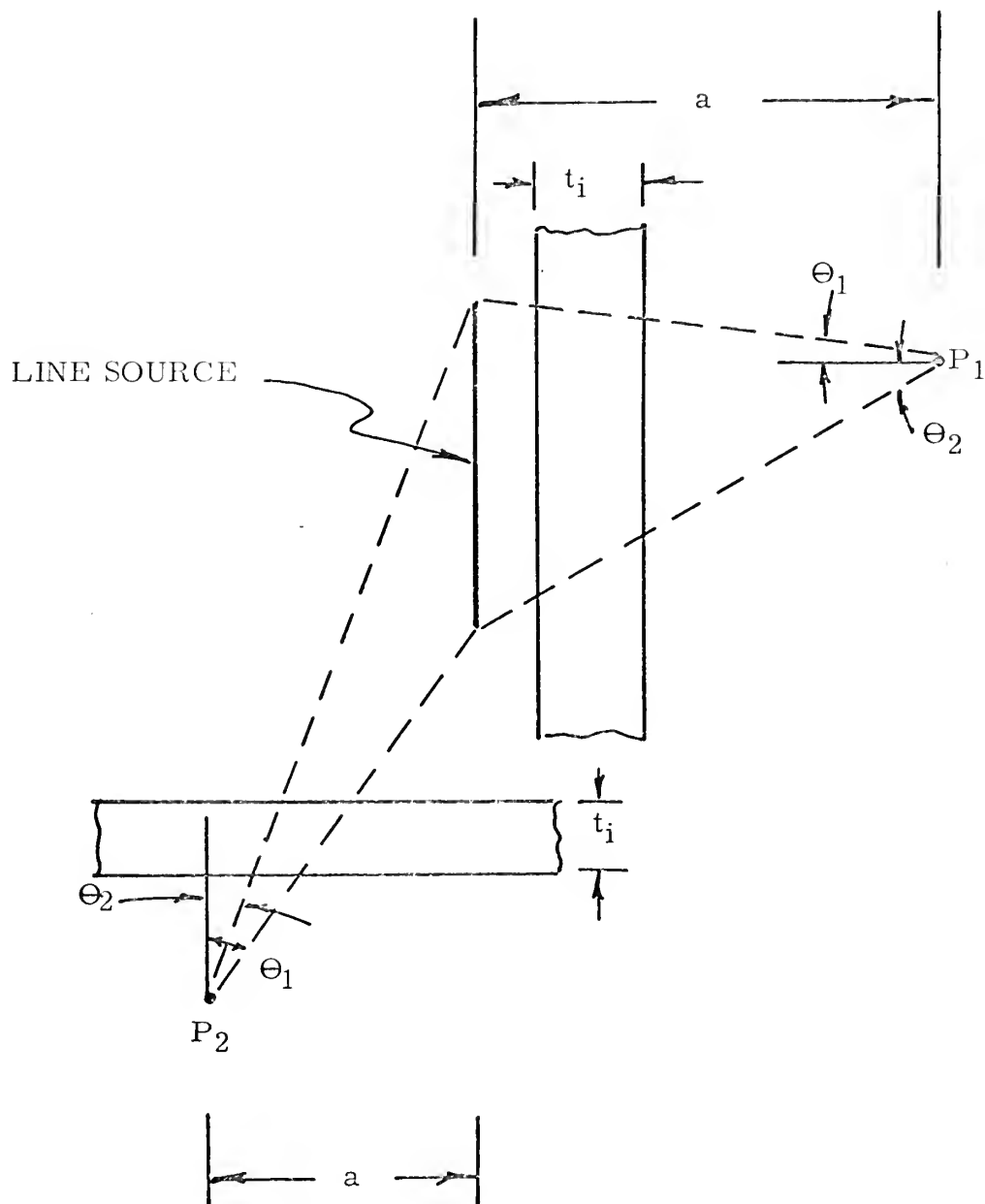
The self-shielding of the fuel element structure, the fuel itself and the other structural members of the generator is not usually included in shielding calculations. (Reference 4.1) However in this design, these self shielding effects are significant and the self shielding of the fuel element and the tungsten emitter heat source are included in the shielding calculations.

The shielding calculations are performed assuming that two 1.25 Mev gammas are emitted for every disintegration of a cobalt-60 atom. The bremsstrahlung radiation resulting from the slowing down of the beta particles is neglected. The geometry of the fuel elements is approximated as line sources located at the center of each fuel element.

#### 4.2 METHOD FOR CALCULATION OF SHIELD THICKNESS

The geometrical arrangement of the gamma source and the shielding is shown in Figure 4.2.1. The dose rate  $D$  at point  $P_1$  is given by equation 4.2.1.





GEOMETRY USED IN THE CALCULATION OF SHIELDING

FIGURE 4.2.1



$$D = \frac{B (1-f) S_L}{a R 4 \pi} [F(\Theta_1, b) + F(\Theta_2, b)] \quad (4.2.1)$$

The dose rate  $D$  at point  $P_1$  is given by equation 4.2.2,

$$D = \frac{B (1-f) S_L}{a R 4 \pi} [F(\Theta_1, b) - F(\Theta_2, b)] \quad (4.2.2)$$

where  $B$  is the dose build up factor, (Reference 4.2),  $f$  is the fraction of emitted gamma radiation absorbed in the fuel (Figure 3.6.1),  $S_L$  is the line source strength in photons/cm-sec.  $R$  is the flux to dose rate conversion factor; it is given in reference 4.3 as a function of gamma energy. The distance  $a$  and the angles  $\Theta_1$  and  $\Theta_2$  are shown in figure 4.2.1.  $b$  is defined in equation 4.2.3.

$$b = \sum_{i=1}^n \mu_i t_i \quad (4.2.3)$$

$t_i$  is the thickness of the shielding material between the source and point  $P$ , and  $\mu_i$  is the macroscopic cross section for gamma attenuation for the shield material.

$$F(\Theta b) = \int_0^{\Theta} e^{-b \sec \Theta'} d\Theta' \quad (4.2.4)$$

$F(\Theta b)$  is plotted as a function of  $b$  for various values of  $\Theta$  in reference 4.3.

All of the quantities in equation 4.2.1 and 4.2.2 are known with the exception of  $b$  and  $F(\Theta b)$ . The equations are thus solved for

$[F(\Theta_1 b) + F(\Theta_2 b)]$  or  $[F(\Theta_1 b) - F(\Theta_2 b)]$  and the value of  $b$  is determined from the graphs in reference 4.3.



### 4.3 SHIELD DESIGN

The components of the system which must be shielded are the five fuel elements. Each fuel element is 10 cm long, 4 cm in diameter and has an  $E_T$  of 1000 watts. The design calls for them to be arranged symmetrically within the tungsten emitter heat source as shown in Figure 4.3.1. They are located exterior to the vacuum housing and, with the exception of one end, are completely surrounded by the tungsten emitter heat source. It is thus necessary to contain all components which are located within the vacuum housing inside the shield. The vacuum housing is a right circular cylinder 23 cm in diameter and 20 cm in height.

Using the line source approximation and the method of calculation described in section 4.2, it was found that a value of  $b$  of 15.5 on the sides of the cylinder and 15 on the ends was required to reduce the dose rate to the desired levels.

The ends of the shield will each be penetrated by five solid rods which are intended to remove heat from the fuel rods on one end and from the thermionic converter collector on the other end. Data from Reference 4.3 indicates that irregularities such as small ducts and iron stiffeners in the shield cause the flux in the vicinity of the irregularity to increase by a factor of 5 to 10 over its value at other areas of the shield. The value of  $b$  for the ends of the shield was therefore increased to 17.5 in order to decrease the flux by an additional factor of 10, since the rods will have an effect similar to the above mentioned irregularities.

Table 4.3.1 lists the values of  $b$  before and after they were modified to account for the self-shielding provided by the tungsten emitter heat source. It also lists the thicknesses of lead and depleted uranium which would be needed to provide the modified value of  $b$ .





## EMITTER HEAT SOURCE

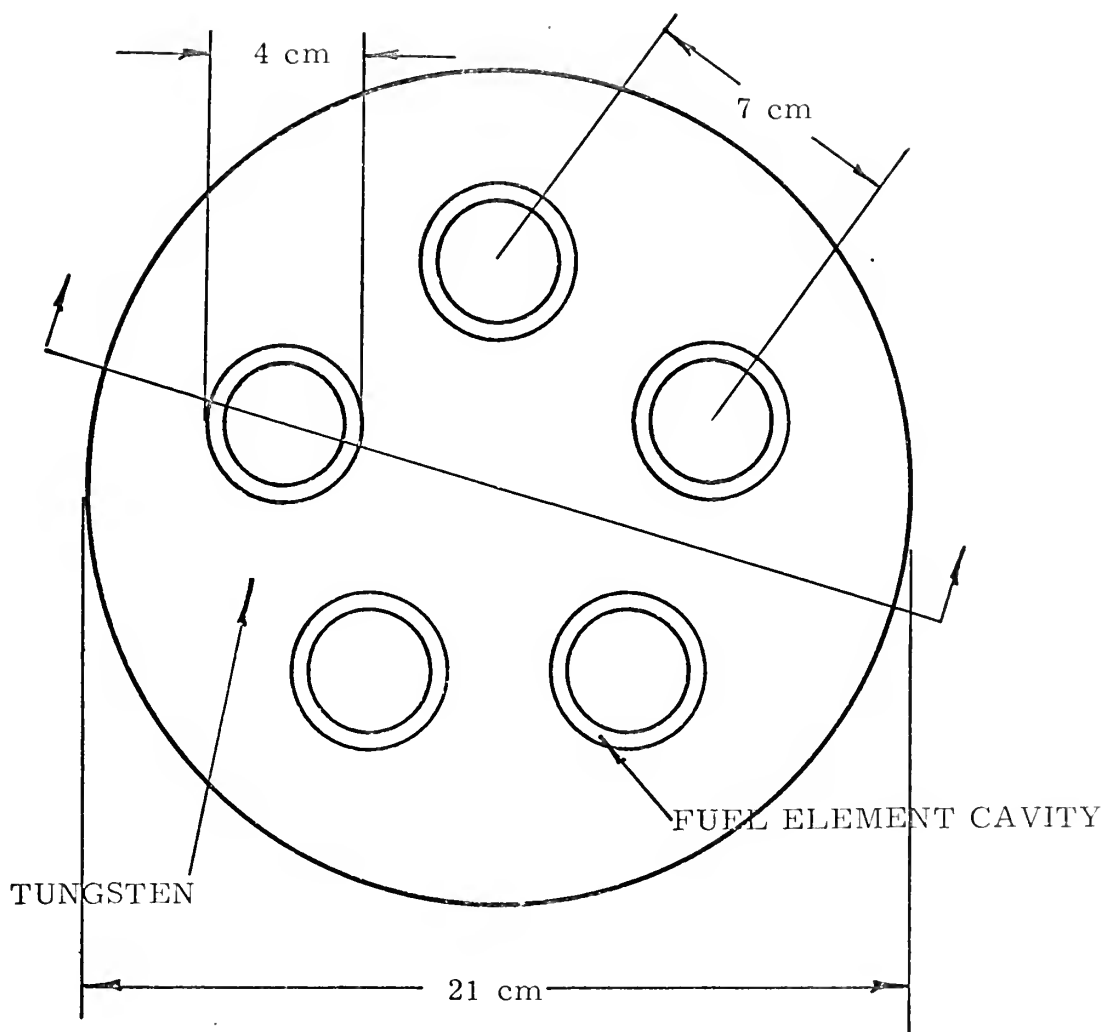


FIGURE 4.3.1



LOCATION	b NO SELF-SHIELDING	b SELF-SHIELDING	LEAD = 11.3 g/cm <sup>3</sup>	URANIUM = 19.08 g/cm <sup>3</sup>
FUEL END	17.5	12.3	19.1 cm	10.5 cm
SIDE	15.5	9.7	15 cm	8.3 cm
CONVERTER END	17.5	8.1	12.5 cm	6.9 cm

REQUIRED SHIELD THICKNESSES

TABLE 4.3.1



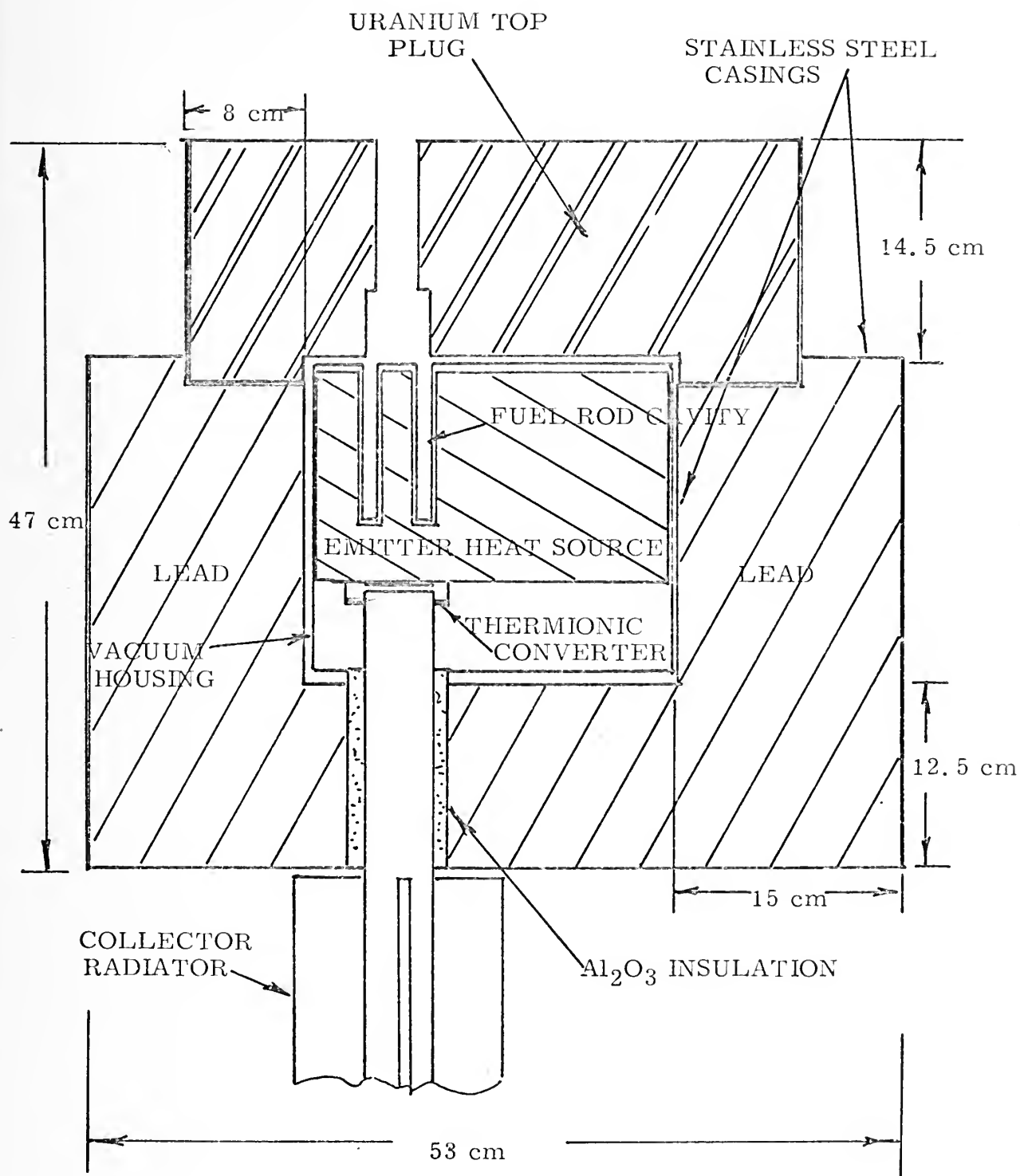
The modified value of  $b$  for the converter end is less than that on the fuel end because there is an additional 4 cm of tungsten between the fuel and the shield on that end.

Lead was selected as the shielding material even though the depleted uranium would have provided a lighter and more compact shield. The relatively low cost and ease with which the lead shield could be fabricated were the basis for this decision.

Due to its low melting point, the lead was not compatible with the power flattening concept incorporated in this design and described in Chapter 5. Thus it was decided to use depleted uranium for the fuel end of the shield. Since wrought depleted uranium has been successfully used as the shielding material for radioisotopic power generators in the SNAP - 7 series, no problem is anticipated with its fabrication. (Reference 4.1) The low melting point of the lead also necessitated insulating the tungsten bars which penetrate the converter end of the shield, from the lead. Aluminum oxide was selected as the insulating material.

A cross section of the shield configuration is shown in Figure 4.3.2. The shield is in the form of a right circular cylinder. The converter end and sides of the shield will be composed of lead. The lead will be cast between an inner and outer casing of stainless steel. The fuel end of the shield will be made of wrought depleted uranium. The lead surface at the lead-uranium interface will be offset to prevent gamma radiation from streaming between the surfaces. The total shield weight is approximately 1040 kg.





CROSS SECTION OF SHIELDED ASSEMBLY

FIGURE 4.3.2





## REFERENCES

- 4.1 Corliss, W.R. and Harvey, D.G., Radioisotopic Power Generation, Englewood Cliffs: Prentice Hall, 1964.
- 4.2 Etherington, H., Nuclear Engineering Handbook, New York: McGraw Hill, 1958.
- 4.3 Rockwell, T., Reactor Shielding Design Manual, Princeton: Van Nostrand Co., 1956.



## CHAPTER 5

### POWER CONDITIONING

#### 5.1 GENERAL REMARKS

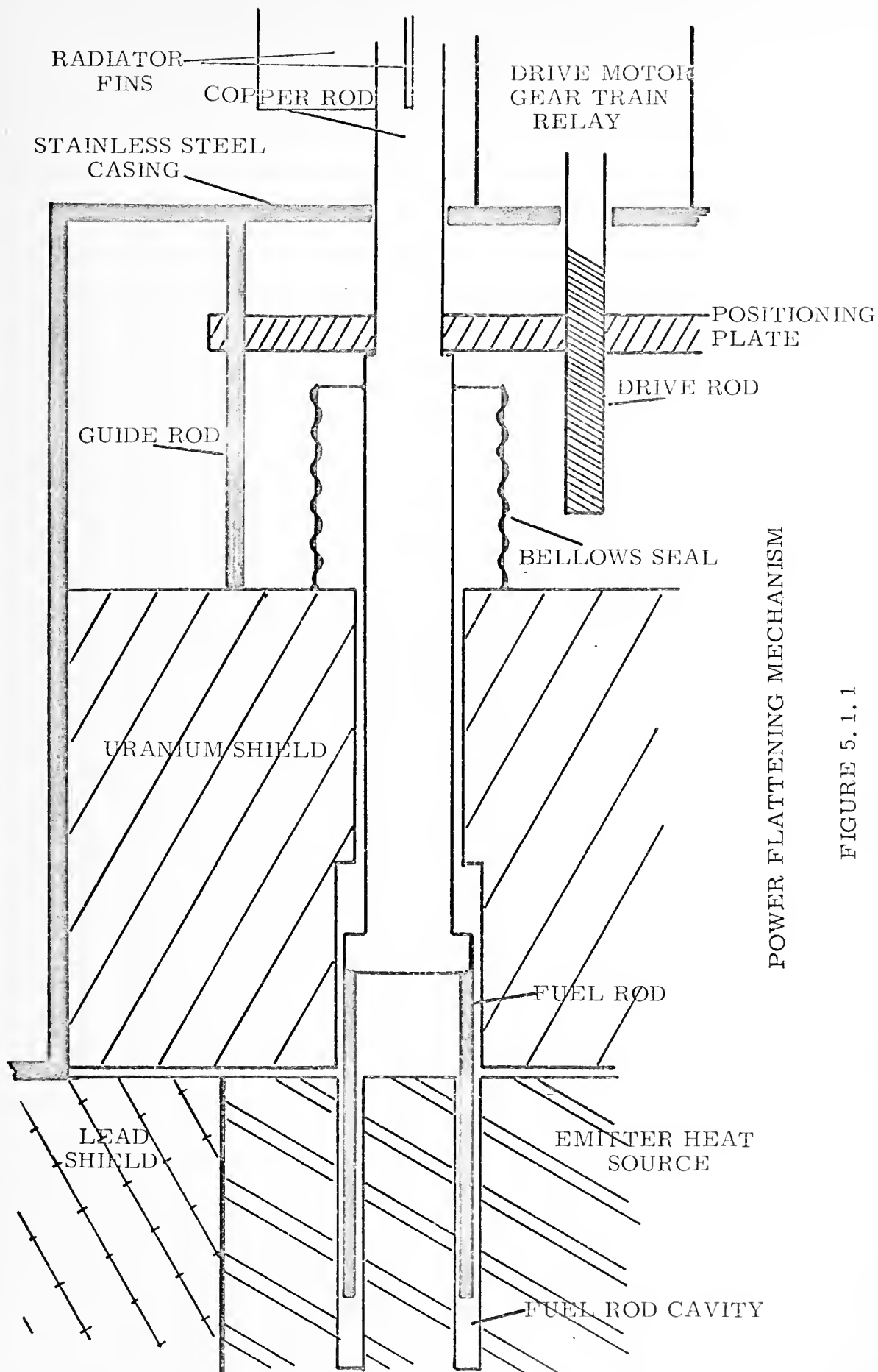
The term power conditioning includes power flattening, voltage transformation and regulation. These topics have been mentioned in preceding chapters and are tied together in this chapter. The design of the power flattening mechanism is treated in detail.

The necessity for power flattening has been discussed in Chapter 2. There it was decided to operate the thermionic converters with a constant power input. This means that the emitter heat source must provide the thermionic emitters with a constant heat flux as the energy available from the decay of the cobalt-60 fuel decreases exponentially with a characteristic half life of 5.25 years.

The thermionic converters can be supplied with a constant power input in two ways. The first method, mentioned in Chapter 2 and the only one to which reference was found in the literature, allows all the energy from the fuel to be deposited in the emitter heat source. A variable heat transfer path is provided to shunt the excess heat from the emitter heat source to the surroundings. As explained in Chapter 2, none of the systems which have been designed to accomplish this objective were practical for this design application.

The second approach, the one used in this design, is to provide a constant energy input to the emitter heat source. Figure 5.1.1 shows the schematic design of a mechanism which is designed to provide the emitter heat source with a constant power input.





POWER FLATTENING MECHANISM

FIGURE 5.1.1



## 5.2 OPERATING PRINCIPLE OF THE POWER FLATTENING MECHANISM

Since the fuel elements are located outside of the vacuum housing, they can be partially withdrawn from the fuel rod cavity in the emitter heat source. As the fuel rod is withdrawn from the fuel rod cavity it will be surrounded by the uranium shield. Most of the gamma radiation from the portion of the fuel rod outside of the emitter heat source will be absorbed by the uranium shield. It is thus possible to vary the energy input to the emitter heat source by varying the position of the fuel rod.

A maximum of 1200 watts of heat will be deposited in the uranium shield. Most of the heat will be deposited in the vicinity of the fuel rods. It will be conducted to the surface of the uranium with a small temperature drop since the uranium provides a path of high thermal conductivity due to its large cross section. The high melting point of the uranium will allow it to operate at a temperature high enough to allow it to be cooled by natural convection.

## 5.3 FUEL ROD POSITIONING MECHANISM

The fuel rod positioning mechanism is shown in Figure 5.1.1. Each of the five copper rods used to conduct heat generated within the fuel rods to the cooling radiators penetrates the uranium shield, passes through and is attached to a movable positioning plate. The rod is then finned to provide sufficient heat transfer area to maintain the fuel rod at a low temperature.

The movable positioning plate is circular in shape, 10 cm in radius, and is attached to each of the five fuel rods as shown in Figure 5.1.1. It is positioned by a threaded drive rod located at its center. As the drive rod is turned the positioning plate travels up or down on it. There





are two guide rods which prevent the positioning plate from exerting a torque on the fuel rods. This torque could cause the fuel rods to bind as they were being moved.

Although the temperature of the fuel rod is considerably lower than the emitter heat source, it would still oxidize quite rapidly if exposed to air. The bellows seals shown in Figure 5.1.1 are employed so that the fuel rods can be maintained in a vacuum or an inert atmosphere. These seals are similar to those used on vacuum system valves and allow the fuel rods to be moved without disturbing the actual seal.

The drive rod is driven through a gear train by an electric motor which is located on the centerline of the assembly as shown in Figure 5.1.1.

#### 5.4 INITIAL FUEL ROD POSITION

The fuel rods are initially positioned so that the output of the system is 500 watts. It would be very difficult to calculate the exact initial position since it would be difficult to determine exactly how much of the gamma radiation emitted from the portion of the fuel located outside of the tungsten emitter heat source eventually reaches the heat source. However, Figure 3.7.2 indicates that most of the gamma energy is absorbed within the first three mean free paths of the material through which it is passing. Therefore a good approximation to the initial position can be obtained by assuming that none of the gamma radiation emitted from the fuel outside of the tungsten emitter heat source reaches it. The error caused by this approximation can be corrected by a slight adjustment of the fuel rod position once the power supply is operating.



From Table 2.3.3.2 it is seen that each of the five thermionic converters requires 510 watts of thermal power. The fuel elements have an  $E_T$  of 1000 watts, an  $\eta_F$  of 75.6% and are 10 cm long. This means that each fuel element supplies 75.6 watts of useful thermal energy per cm of length. Therefore, 6.75 cm of the fuel rod must be inserted into the fuel rod cavity in the emitter heat source. The remaining 3.25 cm of fuel rod will be initially positioned in the uranium shield above the emitter and will gradually be lowered into the fuel rod cavity as the fuel decays. This procedure will allow the energy input to the emitter heat source to be maintained at a constant level.

## 5.5 OPERATION OF THE FUEL POSITIONING MECHANISM

If the thermionic converter power output is allowed to vary 1% the power input can vary 4.5% since the thermionic converter efficiency is 22%. This means that the energy input to each thermionic converter can vary by 23.2 watts which is equivalent to 0.3 cm of fuel rod length.

With this in mind the fuel rod positioning mechanism will operate as follows. When the power output drops below 500 watts a sensing circuit will close a relay and activate the drive motor which will drive the gear train and in turn start lowering the fuel into the fuel rod cavity. One element of the gear train is geared so that it completes one revolution during the time it takes to lower the fuel rod 0.3 cm, at which time it mechanically opens the relay and shuts off the drive motor. This action will be repeated anytime the power output drops below 500 watts.

The frequency with which the fuel will be repositioned can be easily determined. The fraction of fuel which has decayed  $f_F$ , is given by



equation 5.5.1,

$$f_F = 1 - e^{-\lambda t} \quad (5.5.1)$$

where  $\lambda = \frac{\ln 2}{\text{fuel half life}} = 0.132 \text{ yrs}^{-1}$

and  $t$  is the elapsed time in years.

For  $f_F = 0.0454$ , equation 5.5.1 gives  $t$  as 0.35 years; thus the fuel will be repositioned once every 4 months if it is moved 0.3 cm each time. If a smaller variation in power output is required or desired the fuel can be moved a shorter distance at a shorter time interval. This is accomplished simply by modifying the timing of the gear train element which opens the drive motor relay.

## 5.6 VOLTAGE TRANSFORMATION AND REGULATION

The 5 volt output of the five thermionic converters operating in series is transformed to 28 volts by a current drive DC-DC converter as explained in Chapter 2. The DC-DC converter output is coupled to the load through a shunt type voltage regulator. The voltage regulator will maintain a constant voltage output regardless of slight variations in the thermionic converter output caused by the non continuous form of power flattening.

The voltage regulator will also provide the thermionic converters with a constant load; this will allow them to operate at a constant power point even though the power required by the equipment they supply may vary.



## CHAPTER 6

### ADDITIONAL DESIGN CONSIDERATIONS

#### 6.1 GENERAL REMARKS

In this chapter heat loss through the insulation and structural support members of the emitter heat source are discussed. Losses due to the electrical leads are treated. Due to these heat losses a higher input power is required for the same power output. Thus the thermionic converter effectively operates at an efficiency which is lower than the intrinsic efficiency. The effect of these heat losses on the fuel element design and the power flattening mechanism is also discussed.

Several additional problems related to the electrical insulation of the thermionic converters and radiator design, which are peculiar to this design are discussed. These problems are not treated as extensively as the fuel element optimization or the power flattening design. However, they were pursued until it was determined that a practical solution did exist and that they would not prevent construction of a practical thermionic power supply based on this design.

#### 6.2 LEAD LOSSES

Since the thermionic converters in this power supply are connected in series, the emitter of one converter must be connected to the collector of another converter. The heat conducted through the lead from the emitter to the collector is designated  $Q_L$ . This heat loss by the emitter is one of two contributing factors to the lead losses. The second contributing factor is the Joulean heating in the lead,  $Q_J$ . The effect of these losses is to cause the thermionic converter to operate at an efficiency which is lower than its intrinsic efficiency.





The optimum design is not to minimize the sum of  $Q_L$  and  $Q_J$  but to have

$$\dot{Q}_J = \eta_i(Q_L + Q_J) \quad (6.2.1)$$

where  $\eta_i$  is the intrinsic efficiency. The lead losses will depend on the lead material, the lead length to lead area ratio and the temperature difference between the emitter and collector.

In this design  $T_E = 2000^\circ\text{K}$  and  $T_C = 1000^\circ\text{K}$ . Tungsten was chosen for the lead material due to temperature requirements. It was found that equation 6.2.1 was satisfied when the lead length to lead area ratio was 30. The losses are  $Q_L = 42.5$  watts and  $Q_J = 12$  watts, which means that an additional 54.5 watts must be supplied to the emitter. From Figure 2.2.1.3 the emitter output power density at 1.0 volt is found to be  $9.0 \text{ watts/cm}^2$ , thus the area of each emitter must be increased by  $1.3 \text{ cm}^2$  in order to provide the additional 12 watts dissipated as Joulean heating in the lead.

### 6.3 INSULATION AND SUPPORT OF THE EMITTER HEAT SOURCE

The emitter heat source is a right circular cylinder of tungsten. It is 21 cm in diameter, 14 cm in height and weighs 85 kg.

The thermal insulation for the emitter heat source consists of 80 layers of multi-foil insulation similar to that used in the fuel elements. The insulation is 0.9 cm thick and reduces the heat loss from the heat source surface to 110 watts. This insulation is placed inside of the vacuum housing.

If the weight of the emitter heat source was supported by the multi-foil insulation, the foils would be forced together and their insulating properties would be seriously degraded. Therefore pins of zirconium oxide are inserted in holes drilled through the insulation in order to



support the weight that would otherwise rest on the insulation. Conduction by the pins constitutes only a fraction of the total thermal losses associated with the holes in the insulation. The remainder of the heat loss is associated with the thermal short circuiting of the insulation surrounding the pin. (Reference 6.1) The exact value of the heat loss due to the pins would have to be determined experimentally, but Reference 6.1 indicates that for small pins the losses will be on the order of 4 watts per pin. In this design 40 watts is allowed for these pin losses.

Figure 6.3.1 shows the manner in which the pins will be mounted. The pins on the fuel end of the heat source are held tightly in position by disc springs. This mounting technique allows for thermal expansion of the tungsten and keeps the emitter end of the heat source in position. By inserting the pins into recesses in the tungsten, it is possible to prevent any sideways motion of the heat source.

Another heat loss, that due to conduction through the structure of the thermionic converter, has not been calculated since it is very sensitive to the materials used in and the configuration of the thermionic converter casing. A value of 40 watts per converter is used as an estimate of this heat loss.

#### 6.4 MODIFICATIONS REQUIRED TO FUEL ELEMENT DESIGN

The additional heat loss from the emitter heat source due to lead losses and insulation losses totals 622 watts. Thus in order to produce 560 watts of electric power 3162 watts of thermal power must be supplied to the emitter heat source instead of the 2540 watts that would be required if the actual converter operated at the intrinsic efficiency.

The initial fuel loading,  $F_I$  for the design life of  $t$  years is given



by equation 6.4.1,

$$F_I = \frac{P_i}{\eta_F e^{-\lambda t}} \quad (6.4.1)$$

where  $P_i$  is the required thermal power input. For  $P_i = 3162$  and  $t = 3$  years,  $F_I$  is found to be 6250 watts. Therefore the length of each of the five fuel rods must be increased to 12.5 cm giving them an individual  $E_T$  of 1250 watts.

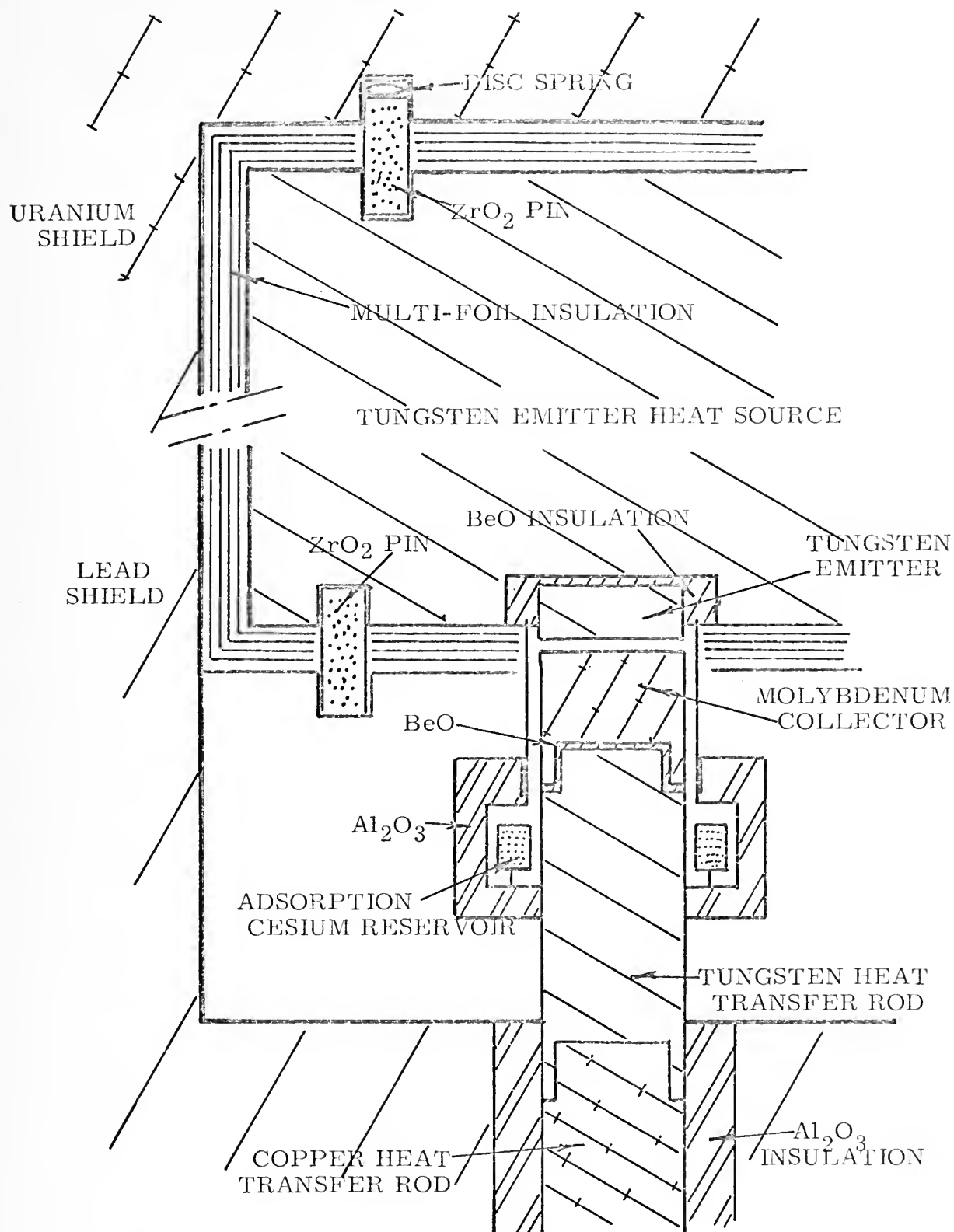
The increased input power requirement makes it necessary to initially position the fuel rod so that an additional 1.65 cm of it are contained within the fuel rod cavity in the emitter heat source. Thus 8.4 cm of the fuel rod will be initially inserted into the fuel rod cavity. Other than a slight increase in the frequency with which the fuel rod is repositioned, the increase in required input power will have no significant effect on the design or operation of the power flattening mechanism.

## 6.5 ELECTRICAL INSULATION OF EMITTER AND COLLECTOR

Since the five thermionic converters mounted on the emitter heat source are electrically connected in series, it is necessary to insure that the only electrical conduction paths between them are the leads connecting the emitters and collectors. The emitters must be electrically insulated from the emitter heat source and the collectors must be insulated from the vacuum housing. Figure 6.5.1 shows where the insulation will be placed in order to accomplish this.

The material used for the electrical insulation must have a reasonably good thermal conductivity. Beryllium oxide was selected as the insulating material because of its relatively high thermal conductivity and high electrical resistivity. Beryllium oxide is stable in an air or vacuum atmosphere to temperatures of at least 2000 °C. (Reference 6.2)





THERMIONIC CONVERTER CONFIGURATION

FIGURE 6.5.1





## 6.6 RADIATOR DESIGN

The radiator used to dissipate the heat deposited at the converter collector must be designed to maintain the collector at  $1000^{\circ}\text{K}$ . The temperature drop in the rod conducting the heat from the collector to the radiator should be minimized in order to allow the radiator to operate at the highest possible temperature. The higher the radiator temperature the smaller its size for a given heat transfer rate.

The heat transfer rod will be composed of tungsten at the collector end and copper at the radiator end. The copper will be used for as much of the rod as the operating temperature allows in order to minimize the temperature drop. The composite heat transfer rod is shown in Figure 6.5.1. If copper is used once the temperature is below  $550^{\circ}\text{C}$  and the rod is 4 cm in diameter the temperature drop in it will be  $270^{\circ}\text{C}$ . The collector radiator will therefore have a maximum temperature of  $460^{\circ}\text{C}$ . In this temperature range radiation and natural convection are the modes of heat transfer which must be considered. Since the temperature distribution in the radiator is difficult to predict, the final radiator design must be determined experimentally.

The design of the radiators associated with the fuel rods is much less critical since it is not necessary to maintain them at a specific temperature but only to insure that they remain at a temperature well below the temperature of the fuel. The copper rods used to conduct heat from the fuel rods to the fuel radiators are the same rods used by the power flattening mechanism to position the fuel rods. The heat conduction rods and fuel radiator are shown in Figure 5.1.1. These rods must remove a maximum of 286 watts from each fuel element. The rods



are 20 cm long and have an average diameter of 3.5 cm. The temperature drop along the rod will therefore be  $150^{\circ}\text{C}$ . If the hottest point on the fuel rod is to be maintained below  $600^{\circ}\text{C}$ , the maximum fuel radiator temperature will be  $150^{\circ}\text{C}$ .



## REFERENCES

- 6.1 Paquin, M.L., "High Temperature Multi-Foil Thermal Insulation," Thermo Electron Corp., Waltham, Mass.
- 6.2 Hove, J.E. and Riley, W.C., Ceramics for Advanced Technologies, New York: John Wiley and Sons, Inc., 1965.



## CHAPTER 7

### SUMMARY AND CONCLUSIONS

#### 7.1 DESIGN SUMMARY

The final power supply design is summarized in Table 7.1.1. The rationale for this design has been given in the preceding chapters. The final design uses five thermionic converters operating at a fixed power point and a DC-DC regulated converter to provide 500 watts of electric power at 28 volts. Although the intrinsic efficiency of the thermionic converters used is 22%, the overall system efficiency is only 9.7%. This decrease in efficiency is due to lead losses, heat lost from the emitter heat source, fuel rod and DC-DC converter inefficiencies.

#### 7.2 CONCLUSIONS

This design shows that it is feasible to build a practical thermionic power supply fueled with cobalt-60. In addition, the power flattening system incorporated in the design enables the operational lifetime of the power supply to be comparable to the half life of cobalt-60.

The fuel element design shows that it is possible to obtain significant savings by using a tubular fuel element instead of a solid fuel rod. In this case there is a 10% increase in the fuel element efficiency, for an  $E_T$  of 1000 watts. Greater savings can be realized for larger values of  $E_T$ .

The major advantage of the cobalt-60 fuel is its relatively low cost. At present strontium-90 is the most popular fuel used for terrestrial radioisotope power supplies with operating periods between one and five years. If it were used in conjunction with the thermionic converters used in this design and if a fuel element efficiency of 95% were realized, 4950





watts of thermal power would have to be provided by the strontium fuel.

At a cost of \$77 per thermal watt (Reference 7.1) the total fuel cost would be \$380,000, as opposed to a cost of \$87,500 for the cobalt-60 fuel. This price differential of \$292,500 is a strong incentive to use cobalt-60 fuel.



TABLE 7.1.1  
FINAL DESIGN SUMMARY

## I THERMIONIC CONVERTERS

Type	High Pressure Cesium Diode
Number of Converters	5
Emitter Material	Tungsten
Emitter Temperature	2000 <sup>o</sup> K
Collector Material	Molybdenum
Collector Temperature	1000 <sup>o</sup> K
Interelectrode Spacing	7 mils
Cesium Reservoir	Internal Adsorption
Cesium Reservoir Temp.	610 <sup>o</sup> K
Output Voltage	1.0 volts
Output Power Density	8.8 watts/cm <sup>2</sup>
Intrinsic Efficiency	22%
Total Power Generated	620 watts
Required Thermal Power Input	2820 watts
Total Emitter Area	70.5 cm <sup>2</sup>

## II FUEL ELEMENTS

Fuel	Cobalt-60
Fuel Form	Metal Wafers
Specific Activity	400 curies/g
Number of Fuel Rods	5
Type of Fuel Element	Tubular
Fuel Rod Length	12.5 cm
Fuel Rod Diameter	4 cm



TABLE 7.1.1 (CONT.)

## III ADDITIONAL HEAT LOSSES

From Emitter Heat Source Through Mult-Foil Insulation	110 watts
Through ZrO <sub>2</sub> Pins	40 watts
From Thermionic Converters Lead Losses	272 watts
Structural Support Losses	200 watts
TOTAL	622 watts

## IV BIOLOGICAL SHIELD

Material	Lead and Depleted Uranium
Total Weight	1040 kg

## V POWER CONDITIONING

Power Flattening	Movable Fuel - Constant Power Input
Voltage Converter	
Type	DC-DC Current Drive
Voltage Input	5 volts
Voltage Output	28 volts
Voltage Regulation	Dissipative Shunt
Efficiency	89%

## VI POWER SUPPLY

Power Output	500 watts
Operational Lifetime	3 years
System Weight	1200 kg
Overall Efficiency	9.7%



## REFERENCES

- 7.1 Corliss, W.R. and Harvey, D.G., Radioisotopic Power Generation, Englewood Cliffs: Prentice Hall, Inc., 1964.





## BIBLIOGRAPHY

- Berger, M.J. and Raso, D.J. "Monte Carlo Calculations of Gamma Ray Backscattering." Radiation Research 12. 20-37. 1960.
- Carvalho, J. and Dunlay, J.B. "Quarterly Progress Report of Research and Development of Vacuum Foil Type Insulation for Radioisotope Power Systems." Thermo Electron Corp. Report No. 4059-109-69. January 20, 1969.
- Corliss, W.R. and Harvey, D.G. Radioisotopic Power Generation. Englewood Cliffs: Prentice Hall, Inc. 1964.
- Dunlay, J.B. "Description of a Cobalt-60 Fueled Thermionic Generator Experiment." Conference Record of the Thermionic Conversion Specialist Conference. October, 1967.
- Etherington, H. Nuclear Engineering Handbook. New York: McGraw Hill. 1958.
- Farace, J.P. "Experimental Cobalt-60 Heat Source Capsules." Savannah River Laboratory. DP-1145.
- Harbaugh, W.E. and Basiulis, A. "The Development of a High-Temperature Reservoir for Automatic Control of Cesium Pressure." Conference Record of the Thermionic Conversion Specialist Conference. November, 1966.
- Hilbom, H.S. "Savannah River Laboratory Isotopic Power and Heat Sources, Part I Co-60." Quarterly Progress Report. July - September, 1967. DP-1129-1.
- Hove, J.E. and Riley, W.C. Ceramics for Advanced Technologies. New York: John Wiley and Sons, Inc. 1965.
- Lingle, J.T. "Energy Source - Low Voltage Conversion System." Proceedings of the 19th Annual Power Sources Conference. 1965.
- Lingle, J.T. "Low Input Voltage Conversion." Proceedings of the 18th Annual Power Sources Conference. May, 1964.
- Lingle, J.T. "Thermionic Low Voltage Converter Regulator Systems." Conference Record of the Thermionic Conversion Specialist Conference. November, 1966.
- Paquin, M.L. "High Temperature Multi-Foil Thermal Insulation." Thermo Electron Corp.
- Rockwell, T. Reactor Shielding Design Manual. Princeton: Van Nostrand Company. 1956.



## BIBLIOGRAPHY (cont.)

- Rush, R.E. and Belofsky, H. "Power Flattening Studies for Radioisotope Thermoelectric Generators." General Instruments Corp. NYO-9783. 1963.
- Storm, M.L., Hurwitz Jr., H. and Roe, G.M. "Gamma Ray Absorption Distributions for Plane, Spherical and Cylindrical Geometries." General Electric Company, Knolls Atomic Power Laboratory. KAPL-783.
- Wilkins, D.R. "A Unified Theoretical Description of Thermionic Converter Performance Characteristics." Journal of Applied Physics. vol. 39. number 5. April, 1968.
- Wilkins, D.R. "An Improved Theoretical Description of Thermionic Converter Performance Characteristics." Proceedings: 27th Annual Physical Electronics Conference. Cambridge, Mass. March, 1967.





thesD634

Design of a cobalt-60 fueled thermionic



3 2768 001 89454 6

DUDLEY KNOX LIBRARY